JOURNAL OF COMPUTATIONAL PHYSICS 36, 366–410 (1980)

Methods for Numerical Conformal Mapping*

RALPH MENIKOFF AND CHARLES ZEMACH

Theoretical Division, Los Alamos Scientific Laboratory, University of California, Los Alamos, New Mexico 87545

Received May 18, 1979; revised September 17, 1979

Nonlinear integral equations for the boundary functions which determine conformal transformations in two dimensions are developed and analyzed. One of these equations has a nonsingular logarithmic kernel and is especially well suited for numerical computations of conformal maps including those which deal with regions having highly distorted boundaries. Numerical procedures based on interspersed Gaussian quadrature for approximating the integrals and a Newton–Raphson technique to solve the resulting nonlinear algebraic equations are described. The Newton–Raphson iteration converges reliably with very crude initial approximations. Numerical examples are given for the mapping of a half-infinite region with periodic boundary onto a half plane, with up to nine-figure accuracy for values of the map function on the boundary and for its first derivatives. The examples include regions bounded by "spike" curves characteristic of Rayleigh–Taylor instability phenomena. A differential equation is derived which relates changes in the map function to changes of the boundary. This is relevant to potential problems for regions with time-dependent boundaries. Further nonsingular integral formulas are derived for conformal mapping in a variety of geometries and for application to the boundary-value problems of potential theory.

I. INTRODUCTION

In many physical problems, a function which is harmonic in a specified region must be determined from its values or normal derivatives on the boundary. In an important subclass of such problems, the main objective is to calculate the boundary values of the function from the boundary normal derivatives, or vice versa. When the region is two dimensional, it can be identified with a region R_z of the complex z plane and complex variable theory can be applied. The harmonic function can be identified with the real or imaginary part of a complex function $f(z)$, analytic in R_z. Because the Laplace equation is conformally invariant, if the conformal mapping of R_z onto a region R_w is known then the solution of the boundary-value problem in R_z can be inferred from that in R_w. The conformal map may have to be determined by numerical rather than analytic means and when the boundary of R_z is specified by discrete numerical data, this is necessarily so.

* Work performed under the auspices of the USDOE. The U.S. Government's right to retain a nonexclusive royalty-free license in and to the copyright covering this paper, for governmental purposes, is acknowledged.

0021-9991/80/090366–45$02.00/0

The current state of the art in numerical conformal mapping is still largely summarized by the books of Gram and Gaier [1]. Some further developments are given by Ives [2] and Hayes *et al.* [3]. As described in these references, the techniques for numerical solution of the equations defining the mapping function work best, if at all, when the shapes of R_z and R_w are similar. If this is not the case, preliminary analytic mappings must be applied to bring R_z into suitable shape before the numerical work is undertaken. For example, if an airfoil is to be mapped onto a circle, the airfoil must first be "premapped" onto an approximately circular region by a device such as the von Karman–Trefftz transformation, or even a series of such devices.

The present work was motivated by the authors' study of the Rayleigh–Taylor instability of the interface between two irrotational incompressible fluids. The fluid flow is governed by velocity potentials determined from data on the fluid interface. The velocity potentials are harmonic functions. Because the interface changes in time, the potential problem must be recalculated at each time step in the evolution of the system. The interface may become quite distorted in shape. Moreover, a small fluctuation in the shape of the interface can grow quite rapidly. Rapid growth of such fluctuations may appear in a numerical calculation regardless of whether they are due to physical assumption or mathematical inaccuracy. Thus, whatever technique is applied to the potential problem for hydrodynamic systems of this character faces severe tests with regard to accuracy, computer speed, and applicability to distorted regions.[1]

II. Formulations

The questions addressed in this paper can be grouped in three categories:

(1) First, suppose $F(w)$ is a function of the complex variable w, $w = u + iv$, and is analytic in a region R_w of the w plane. Let its real and imaginary parts be $F_R(u, v)$ and $F_I(u, v)$. If R_w is unbounded, suppose also that as $w \to \infty$ within the region

$$F(w) \to F(\infty) + O(|\, w \,|^{-1}),$$

where $F(\infty) = F_R(\infty) + iF_I(\infty)$ is a constant, not necessarily equal to zero. One may ask how to determine the function $F(w)$ in R_w if either F_R or F_I is specified along its boundary. One approach is to use Cauchy's formula to express $F(w)$ as an integral over the boundary. If the integrand is properly chosen, boundary values of either F_R or F_I (but not both) will contribute. As a limiting case, the values of F_R (or F_I) on the boundary are given in terms of a boundary integral depending on F_I (or F_R). The integrand has a pole singularity and the integration is of the principal value type. An integration by parts can transform this into an integral with a logarithmic singularity in the integrand. An alternative is to apply one of Green's theorems to the harmonic

[1] For an alternative approach to numerical potential theory dealing directly with Green's integral equations, see [4]. Also, see [5] for an alternative mapping technique based on the Schwarz–Christoffel formula. We thank the reviewer for this citation.

functions F_R or F_I, in conjunction with a Green's function for R_w. This leads to integrals along the boundary with logarithmically singular integrands, from which the principal value integrals can be obtained by integration by parts.

(2) Second, suppose a region R_z in the complex z plane, $z = x + iy$, is given and an analytic function $z = z(w)$ (or perhaps $w = w(z)$) is sought which maps R_w conformally onto R_z. This can be regarded as an application of (1). A variety of nonlinear integral equations relating the boundary values of $x(u, v)$, $y(u, v)$ (or $u(x, y)$, $v(x, y)$) can be developed. With regard to the applications we have studied, the most useful equations seem to be those carrying the logarithmic singularities. The most practical method for evaluating these integrals seems to be a combination of quadrature rules of the Gaussian type (open rules) and of the Gauss–Lobatto type (closed rules). We shall refer to this as the technique of "interspersed Gaussian quadrature." It leads to nonlinear algebraic equations which can be solved by the Newton–Raphson method. The main task of the present paper is to explain these procedures.

(3) Third, let $f(x, y)$ be a harmonic function defined in the region R_z. One may ask how to determine $f(x, y)$ from values of f or values of the normal derivatives $\partial f/\partial n$ on the boundary, and also, how the boundary values of f and $\partial f/\partial n$ codetermine each other. These questions can be answered by application of (1) and (2) above.

The remainder of this paper is divided into two parts. In Part A, we analyze the three cited questions in a context which we call *even-periodic geometry*. This refers to functions $F(w)$ such that $F_R(u, v)$ is periodic and even in the u-variable. It also refers to regions R_z with boundary specified by $y = \hat{y}(x)$, where $\hat{y}(x)$ is periodic and even in x. For the purposes of this paper, a periodic function will always have period 2π. This was the class of problems encountered first in our Rayleigh–Taylor study. Accordingly, we develop here a structure of theoretical formulas and numerical analysis for which a fair quantity of illustrative numerical results can also be reported.

In Part B, we seek to round out the discussion by extending the results to other geometries closely related to even-periodic geometry. This permits contact with existing formalisms, e.g., those that map a closed region onto a circle. This context will be called circle geometry. No numerical experiments are described for these cases. However, the analogy to Part A is quite close and we believe the methods applied there should be equally effective in the geometries of Part B.

In Section III, a set of integral formulas is obtained interrelating F_R and F_I on the relevant boundary of R_w for even-periodic geometry; this is the interval $0 \leqslant u \leqslant \pi$ of the u-axis. Three nonlinear integral equations defining the conformal mapping problem in this setting are obtained, both in singular and in nonsingular form. Formulas for solving the boundary-value problem for harmonic functions are also given.

In Section IV, the technique for solving the third of these integral equations for the mapping problem in terms of interspersed Gaussian quadrature rules is described in detail. In Section V, accuracy and rates of convergence of the method are discussed in terms of specific examples.

In Section VI, a differential approach to the mapping problem is undertaken. This provides a linear relation between a small change in the boundary and the resultant small change in the mapping function. When the boundaries of a physical system change in time, the consequent changes in the mapping function can be inferred from a set of differential equations in the time variable.

In Sections VII and VIII (in Part B), analogs of these results are obtained for periodic and circle geometries. One of the variants that emerges is the already well-known equation of Theodorsen and Garrick [1]. The key equations when the region R_w of interest is a half-plane (linear geometry) are briefly noted in Section IX.

Depending on the geometry under consideration, the regions R_w will be taken as upper-half planes (rather than lower), or exteriors of circles (rather than interiors). The transformation $F(w) \to F^*(w^*)$ carries a function analytic in a portion of the upper-half plane into a function analytic in the corresponding portion of the lower-half plane. The transformation $F(w) \to F^*(1/w^*)$ carries a function analytic in the exterior of the unit circle into a function analytic in the interior. On the boundaries of their respective domains, these transformation carry F_R into $+F_R$ and F_I into $-F_I$. By these rules, any equations explicitly treated in this paper can be easily replaced by equations applicable to the complementary regions.

Lastly, we note that the mapping of certain types of irregular regions has not been addressed in this paper. For example, the boundary curve $y = \hat{y}(x)$ referred to above will be understood to be single valued. If, in fact, the boundary "doubles back" on itself several resorts are possible. One could base the parametrization of the boundary and the quadrature rules on a more convenient parameter such as arc length, or one could introduce a suitable premap. The relative merits of such alternatives may vary from case to case, and their appraisal is left for another study. In our examples, $\hat{y}(x)$ is also differentiable, but this is not an essential limitation to the method.

PART A

III. Even-Periodic Geometry

1. *Preliminaries*

Let R_w denote the upper-half strip of the w plane defined by $0 \leqslant u \leqslant \pi$, $0 \leqslant v < \infty$. Let $F(w)$ be analytic in the upper-half w plane (and, in particular, in the interior of R_w). As already prescribed in Section II, we denote its real and imaginary parts as $F_R(u, v)$ and $F_I(u, v)$, and assume that as $w \to \infty$ in R_w, $F(w)$ approaches a constant $F(\infty)$ to order $|w|^{-1}$. $F(w)$ will be called an even-periodic function if it satisfies two conditions:

$$F(w) = F^*(-w^*), \tag{3.1a}$$

$$F(w) = F(w + 2\pi). \tag{3.1b}$$

The first condition implies

$$F_R(u, v) = F_R(-u, v),$$
$$F_I(u, v) = -F_I(-u, v),$$
$$F(\infty) = F_R(\infty) = \text{real}.$$

Moreover, both F_I and $\partial F_R/\partial u$ vanish at $u = 0$ and $u = \pi$, for $v > 0$.

Under suitable regularity conditions, F_R and F_I have the Fourier expansions

$$F_R(u, v) = F_R(\infty) + \sum_{n=1}^{\infty} a_n e^{-nv} \cos nu,$$

$$F_I(u, v) = \sum_{n=1}^{\infty} a_n e^{-nv} \sin nu,$$

where the coefficients $\{a_n\}$ are real. This indicates that $F(w)$ should be completely determined by specifying F_R for $v = 0$, or by specifying F_I for $v = 0$ and $F_R(\infty)$.

Let w and w' be restricted to the interior of R_w. Then $(\cos w - \cos w')$ vanishes only at $w = w'$, and $(\cos w^* - \cos w')$ cannot vanish. By Cauchy's theorem,

$$F(w) = \frac{\sin w}{2\pi i} \int_C \frac{F(w')}{\cos w - \cos w'} \, dw' \tag{3.2a}$$

and

$$0 = \int_C \frac{F(w')}{\cos w^* - \cos w'} \, dw', \tag{3.2b}$$

where C is any closed contour in R_w which encircles w counterclockwise. Take C along the boundary of R_w. The upper horizontal part of C is along $v = v_\infty$, with the understanding that the limit $v_\infty \to \infty$ will be taken. We can also write

$$F(w) = \frac{1}{2\pi i} \int_C \frac{\sin w' F(w')}{\cos w - \cos w'} \, dw' \tag{3.3a}$$

and

$$0 = \int_C \frac{\sin w' F(w')}{\cos w^* - \cos w'} \, dw'. \tag{3.3b}$$

In the next subsection, we encounter integrals over the interval $0 \leqslant u \leqslant \pi$ whose integrands become singular when the parameter w approaches a real value u. A basic rule for this situation is expressed by

$$\lim_{\epsilon \to 0} \frac{1}{u - u' + i\epsilon} = \text{p.v.} \frac{1}{u - u'} - \pi i \, \delta(u - u') \, \text{sign}(\epsilon),$$

where p.v. stands for principal value and $\delta(u - u')$ denotes the Dirac delta function. The relation is to be applied under an integral sign.

Then if w approaches the real value u from the interior of R_w and $0 \leqslant u' \leqslant \pi$, we find

$$\lim_{w \to u} \frac{\sin w}{\cos w - \cos u'} = \text{p.v.} \frac{\sin u}{\cos u - \cos u'} + \pi i \, \delta(u - u') \tag{3.4a}$$

and, similarly,

$$\lim_{w \to u} \frac{\sin u'}{\cos w - \cos u'} = \text{p.v.} \frac{\sin u'}{\cos u - \cos u'} + \pi i \, \delta(u - u'). \tag{3.4b}$$

There are companion rules for differentiation under an integral sign:

$$\frac{d}{du'} \log | \cos u - \cos u' | = \text{p.v.} \frac{\sin u'}{\cos u - \cos u'}, \tag{3.5a}$$

$$\frac{d}{du'} \log \left| \frac{\sin \frac{1}{2}(u - u')}{\sin \frac{1}{2}(u + u')} \right| = \text{p.v.} \frac{\sin u}{\cos u - \cos u'}, \tag{3.5b}$$

where it is noted that the arguments of the (natural) logarithms are absolute values.

2. *Representations of $F(w)$ in Terms of Boundary Values*

Combining (3.2a) and (3.2b), we get

$$F(w) = \frac{\sin w}{2\pi i} \left\{ \int_C \frac{F(w') \, dw'}{\cos w - \cos w'} + \left[\int_C \frac{F(w') \, dw'}{\cos w^* - \cos w'} \right]^* \right\}.$$

The upper horizontal part of the contour C is now allowed to recede to infinity while the other parts approach the boundaries of R_w. We find

$$F(w) = -i \sin w \int_0^\pi \frac{F_R(u', 0)}{\cos w - \cos u'} \frac{du'}{\pi}. \tag{3.6a}$$

Proceeding in a similar way from (3.3a) and (3.3b), we have

$$F(w) = \frac{1}{2\pi i} \left\{ \int_C \frac{\sin w' \, F(w') \, dw'}{\cos w - \cos w'} - \left[\int_C \frac{\sin w' \, F(w') \, dw'}{\cos w^* - \cos w'} \right]^* \right\},$$

whence

$$F(w) = F_R(\infty) + \int_0^\pi \frac{\sin u' \, F_I(u', 0)}{\cos w - \cos u'} \frac{du'}{\pi}. \tag{3.6b}$$

Equations (3.6a) and (3.6b) are the desired relations. They show how over the whole of R_w, $F(w)$ can be determined from knowledge either of $F_R(u, 0)$ or of $F_I(u, 0)$ and the (real) constant $F_R(\infty)$.

Also, if we let $\mathrm{Im}(w) \to +\infty$ in (3.6a), we get

$$F_R(\infty) = \int_0^\pi F_R(u', 0) \frac{du'}{\pi}. \tag{3.7}$$

3. *Integral Relations among Boundary Values*

For u real and $0 \leqslant u \leqslant \pi$, we can relate $F_I(u, 0)$ to $F_R(u, 0)$ by taking the limit $w \to u$ and applying (3.4a). The real part of the resulting equation is an identity: the imaginary part reads:

$$F_I(u, 0) = -\sin u \text{ p.v.} \int_0^\pi \frac{F_R(u', 0)}{\cos u - \cos u'} \frac{du'}{\pi}. \tag{3.8a}$$

Conversely, we can relate $F_R(u, 0)$ to $F_I(u, 0)$ by using (3.6b) and (3.4b). This gives

$$F_R(u, 0) = F_R(\infty) + \text{p.v.} \int_0^\pi \frac{\sin u' \, F_I(u', 0)}{\cos u - \cos u'} \frac{du'}{\pi}. \tag{3.8b}$$

Equations (3.8a) and (3.8b) are sometimes called finite Hilbert transforms. If these integrals are integrated by parts with the aid of (3.5), the contributions at the end points vanish and we have

$$F_I(u, 0) = \int_0^\pi \log \left| \frac{\sin \frac{1}{2}(u - u')}{\sin \frac{1}{2}(u + u')} \right| \frac{\partial F_R(u', 0)}{\partial u'} \frac{du'}{\pi}, \tag{3.9a}$$

$$F_R(u, 0) = F_R(\infty) - \int_0^\pi \log |\cos u - \cos u'| \frac{\partial F_I(u', 0)}{\partial u'} \frac{du'}{\pi}. \tag{3.9b}$$

A large family of definite integral formulas can be generated from (3.8a) and (3.8b) by choosing suitable functions $F(w)$. Here, we only note two consequences of choosing $F(w) = 1$.

First, Eq. (3.8a) yields the (well-known) result

$$\sin u \text{ p.v.} \int_0^\pi \frac{1}{\cos u - \cos u'} \frac{du'}{\pi} = 0. \tag{3.10}$$

Second, from Eq. (3.6a),

$$\int_0^\pi \frac{\sin w}{\cos w - \cos u'} \frac{du'}{\pi} = i. \tag{3.11}$$

Integrating this with respect to w from w_1 to w_2 and then letting $\mathrm{Im}(w_2) \to \infty$, we have

$$\int_0^\pi \log(\cos w_1 - \cos u') \frac{du'}{\pi} = i(w_2 - w_1) + \int_0^\pi \log(\cos w_2 - \cos u') \frac{du'}{\pi}$$

$$\to -iw_1 - \log 2 \tag{3.11a}$$

after the limit on w_2 is taken. Finally, letting $w_1 \to u$ = real, and taking the real part, we get the curious but useful formula

$$\int_0^\pi \log |\cos u - \cos u'| \frac{du'}{\pi} = -\log 2. \tag{3.12}$$

4. *Integral Equations for Conformal Mapping*

Let there be a curve in the complex z plane defined by $y = \hat{y}(x)$. Suppose that for all x, $\hat{y}(x + 2\pi) = \hat{y}(x)$ and $\hat{y}(-x) = \hat{y}(x)$. A real function $\hat{y}(x)$ with these properties will also be termed even periodic. We shall presume that $\hat{y}(x)$ is everywhere differentiable, though this condition can be relaxed.

Let $z = z(w)$ be a function analytic in the upper half w plane which conformally maps this upper half plane into the portion of the z plane above $y = \hat{y}(x)$ and carries $w = i\infty$ into $z = i\infty$. Let this mapping be standardized by setting $x = 0, \pi$ for $u = 0, \pi$, respectively. The mapping can be represented as

$$z = z(w) = w + iF(w), \tag{3.13}$$

where $F(w)$ is an even-periodic analytic function in the upper-half w plane. Then

$$x = x(u, v) = u - F_I(u, v), \tag{3.13a}$$

$$y = y(u, v) = v + F_R(u, v). \tag{3.13b}$$

We shall abbreviate $x(u, 0)$ and $y(u, 0)$ to $x(u)$ and $y(u)$, respectively, and write $u(x)$ for the function inverse to $x(u)$. These expressions will maintain these meanings throughout the paper. Then for $v = 0$, we have

$$x = x(u) = u - F_I(u, 0), \tag{3.14a}$$

$$y = y(u) = F_R(u, 0), \tag{3.14b}$$

as parametric equations, with parameter u, of $y = \hat{y}(x)$. To study these functions, it is sufficient to restrict our attention to the region R_w of the w plane and the image region R_z of the z plane. The equations of the previous subsection are applicable with $F_R(u, 0) = y(u)$, $F_I(u, 0) = -[x(u) - u]$. Let $\lim_{v\to\infty} F_R(u, v)$, previously called $F(\infty)$, be here denoted by y_∞. Then

$$x(u) = u + \sin u \text{ p.v.} \int_0^\pi \frac{y(u')}{\cos u - \cos u'} \frac{du'}{\pi} \tag{3.15}$$

and

$$y(u) = y_\infty - \text{p.v.} \int_0^\pi \frac{\sin u'[x(u') - u']}{\cos u - \cos u'} \frac{du'}{\pi}. \tag{3.16}$$

With the function $\hat{y}(x)$ specified as the input, and taking into account that

$$y(u) = \hat{y}(x(u)), \tag{3.17}$$

either of the equations (3.15) or (3.16) constitutes a nonlinear integral equation for the unknown function $x(u)$. If (3.16) is the equation employed, y_∞ is also unknown, but can be expressed in terms of $x(u)$ by evaluating (3.16) either at $x = u = 0$ or at $x = u = \pi$; e.g.,

$$\hat{y}(0) = y_\infty - \int_0^\pi \frac{\sin u'[x(u') - u']}{1 - \cos u'} \frac{du'}{\pi} . \tag{3.18}$$

In (3.18), the integrand is not singular at $u' = 0$, but reduces to $(2/\pi)(dx/du - 1)_{u=0}$.

An alternate equation can be derived starting with Eq. (3.9b):

$$y(u) = y_\infty + \int_0^\pi \log | \cos u - \cos u' | \left(\frac{dx(u')}{du'} - 1\right) \frac{du'}{\pi} .$$

The integral here is seen to separate into two terms. In the first term, it is more convenient to take the x variable as the independent variable, writing $u' = u(x')$, $u = u(x)$, and replacing $y(u)$ by the equivalent $\hat{y}(x)$. In the second term, Eq. (3.12) applies. We find that

$$\hat{y}(x) = y_\infty + \log 2 + \int_0^\pi \log | \cos u(x) - \cos u(x')| \frac{dx'}{\pi} , \tag{3.19}$$

which is a nonlinear integral equation for the unknown function $u(x)$ and the unknown constant y_∞ when $\hat{y}(x)$ is specified. The constant y_∞ can be eliminated by, e.g., subtracting from (3.19) the same equation evaluated at $x = u(x) = 0$:

$$\hat{y}(x) = \hat{y}(0) + \int_0^\pi \log \left| \frac{\cos u(x) - \cos u(x')}{1 - \cos u(x')} \right| \frac{dx'}{\pi} . \tag{3.20}$$

However, we prefer to retain y_∞ explicitly up to the stage of numerical computation.

Equation (3.19) must be supplemented with the conditions $u(0) = 0$ and $u(\pi) = \pi$ in order to define a unique solution. Otherwise, the transformations

$$\cos u(x) \to a \cos u(x) + b, \; y_\infty \to y_\infty - \log a$$

would generate a multiplicity of solutions.

For the numerical solution of the integral equations (3.15), (3.16), or (3.19), some rule for approximate evaluation of the integral will be required; to this end, it is desirable to reexpress the integrals in nonsingular form. Referring to Eq. (3.10) and again to Eq. (3.12), we see that the three integral equations can be regularized as follows:

$$x(u) = u + \sin u \int_0^\pi \frac{y(u') - y(u)}{\cos u - \cos u'} \frac{du'}{\pi} , \tag{3.21}$$

$$y(u) = y_\infty - \int_0^\pi \frac{\sin u'[x(u') - u'] - \sin(u)[x(u) - u]}{\cos u - \cos u'} \frac{du'}{\pi} , \tag{3.22}$$

$$\hat{y}(x) = y_\infty + \int_0^\pi \log \left| \frac{\cos u(x) - \cos u(x')}{\cos x - \cos x'} \right| \frac{dx'}{\pi} . \tag{3.23}$$

There is a more general method of regularizing Eq. (3.19). Suppose that for the curve $y = \hat{y}_0(x)$, the solution $\{u_0(x), (y_0)_\infty\}$ to (3.19) is known. Then by comparing the equations for each case, we obtain

$$\hat{y}(x) - \hat{y}_0(x) = y_\infty - (y_0)_\infty + \int_0^\pi \log \left| \frac{\cos u(x) - \cos u(x')}{\cos u_0(x) - \cos u_0(x')} \right| \frac{dx'}{\pi}.$$

This can be regarded as comparing the conformal map for the curve $\hat{y}(x)$ to that of $\hat{y}_0(x)$. Equation (3.23) corresponds to the special case in which $\hat{y}_0(x) = (y_0)_\infty = 0$ and $u_0(x) = x$.

The key theoretical result of the present section is the third integral equation of this list, Eq. (3.23). This is the one that yielded the most satisfactory results, by procedures that will be detailed in the next section. The first two equations also yielded good results, provided the amplitude of the $\hat{y}(x)$ curve and its maximum slope are not too large.

Hereafter, the function $u(x)$ will be called the *boundary map function* associated with the conformal transformation $z = z(w)$ defined by $\hat{y}(x)$. Further, its inverse $x(u)$ will be called the inverse boundary map function. The determination of $u(x)$ is the key to the determination of all other features of the conformal map.

An additional integral equation can be inferred from (3.9a); this one would suggest use of y as the independent variable. We have not investigated this equation.

5. *Relations among Harmonic Functions, Their Boundary Values and Boundary Normal Derivatives*

Suppose that $f(x, y)$ satisfies the Laplace equation

$$(\partial_x^2 + \partial_y^2) f(x, y) = 0$$

in the region of the z plane lying above the boundary curve $y = \hat{y}(x)$ where $\hat{y}(x)$ is even periodic. Suppose $f(x, y)$ is even periodic in the x variable. Then $\partial_x f(x, y) = 0$ for $x = 0, \pi$. Let $f(x)$, $f_s(x)$, and $f_n(x)$ represent the function and its tangential and normal derivatives along the boundary. The tangential derivative is taken in the direction of increasing x and the normal derivative is taken *into* the region of definition. Then

$$f(x) = f(x, \hat{y}(x)), \tag{3.24}$$

$$f_s(x) = \left[\frac{\partial f(x, y)}{\partial x} + \frac{d\hat{y}(x)}{dx} \frac{\partial f(x, y)}{\partial y}\right]_{y=\hat{y}(x)} \Big/ [1 + (d\hat{y}/dx)^2]^{1/2}, \tag{3.25a}$$

$$f_n(x) = \left[-\frac{d\hat{y}(x)}{dx} \frac{\partial f(x, y)}{\partial x} + \frac{\partial f(x, y)}{\partial y}\right]_{y=\hat{y}(x)} \Big/ [1 + (d\hat{y}/dx)^2]^{1/2}. \tag{3.25b}$$

It is also useful to define a modified normal derivative $f_{nsq}(x)$ by

$$f_{nsq}(x) = \left[-\frac{d\hat{y}}{dx} \frac{\partial f}{\partial x} + \frac{\partial f}{\partial y}\right]_{y=\hat{y}(x)} = f_n(x)[1 + (d\hat{y}/dx)^2]^{1/2}. \tag{3.26a}$$

A companion equation to this one is given by differentiating f:

$$\frac{df(x)}{dx} = \left[\frac{\partial f}{\partial x} + \frac{d\hat{y}}{dx}\frac{\partial f}{\partial y}\right]_{y=\hat{y}(x)} = f_s(x)[1 + (d\hat{y}/dx)^2]^{1/2}. \tag{3.26b}$$

We seek integral equations interrelating $f(x)$, $f_s(x)$, $f_n(x)$, or equivalently, $f(x)$, $df(x)/dx$, $f_{nsq}(x)$ and expressions for $f(x, y)$ in terms of them. The first step is to reformulate the problem in the w plane.

Let $z = z(w)$ be the conformal map which carries the upper-half w plane into the z plane above $y = \hat{y}(x)$ as detailed in the previous subsection. Let $\bar{f}(u, v)$ be the transform of $f(x, y)$ as defined by

$$\bar{f}(u, v) = f(x(u, v), y(u, v)). \tag{3.27}$$

Then $\bar{f}(u, v)$ is a harmonic function, and satisfies the Laplace equation

$$(\partial_u{}^2 + \partial_v{}^2)\bar{f}(u, v) = 0.$$

We define the boundary functions $\bar{f}(u), \bar{f}_s(u), \bar{f}_n(u)$ by

$$\bar{f}(u) = \bar{f}(u, 0), \tag{3.28}$$

$$\bar{f}_s(u) = \frac{\partial \bar{f}(u, 0)}{\partial u}, \tag{3.29a}$$

$$\bar{f}_n(u) = \left[\frac{\partial \bar{f}(u, v)}{\partial v}\right]_{v=0}. \tag{3.29b}$$

It follows that, with the map of the boundary specified as above by $x = x(u)$, or inversely, by $u = u(x)$,

$$\bar{f}(u) = f(x), \tag{3.30}$$

$$\bar{f}_s(u) = \frac{df(x)}{dx}\left(\frac{du(x)}{dx}\right)^{-1}, \tag{3.31a}$$

$$\bar{f}_n(u) = f_{nsq}(x)\left(\frac{du(x)}{dx}\right)^{-1}. \tag{3.31b}$$

Consider the function $F(w)$ defined by

$$F(w) = -i \sin w \int_0^\pi \frac{\bar{f}(u')}{\cos w - \cos u'}\frac{du'}{\pi}. \tag{3.32}$$

Then $F(w)$ is verified to be even-periodic analytic function in the upper-half w plane. Taking the limit $v \to \infty$, we have

$$F(\infty) = \int_0^\pi \bar{f}(u')\frac{du'}{\pi}.$$

The considerations of subsection III.2 follow. The function $\bar{f}(u, v)$ solving the Laplace equation in the w plane and having $\bar{f}(u)$ as a boundary value is identified as $F_R(u, v)$. Moreover, the function $i\,dF(w)/dw$ is even periodic when $F(w)$ is. Its boundary value is

$$i\left[\frac{dF(w)}{dw}\right]_{v=0} = -\frac{\partial F_I(u, 0)}{\partial u} + i\frac{\partial F_R(u, 0)}{\partial u} = \bar{f}_n(u) + i\bar{f}_s(u). \tag{3.33}$$

By (3.32),

$$\lim_{v\to\infty} i\frac{dF(w)}{dw} = 0.$$

Applying Eq. (3.9b) to $F(w)$, applying (3.8) to $i\,dF(w)/dw$, and converting via (3.31) and $du' = (du(x')/dx')\,dx'$ to integrations in the z plane, we get the list of boundary equations:

$$f(x) = f_\infty + \int_0^\pi \log|\cos u(x) - \cos u(x')|\, f_{nsq}(x')\frac{dx'}{\pi}, \tag{3.34}$$

$$\frac{df(x)}{dx} = -\frac{du(x)}{dx}\sin u(x)\ \text{p.v.}\int_0^\pi \frac{f_{nsq}(x')}{\cos u(x) - \cos u(x')}\frac{dx'}{\pi}, \tag{3.35a}$$

$$f_{nsq}(x) = \frac{du(x)}{dx}\ \text{p.v.}\int_0^\pi \frac{\sin u(x')(df(x')/dx')}{\cos u(x) - \cos u(x')}\frac{dx'}{\pi}. \tag{3.35b}$$

Here,

$$f_\infty = \lim_{y\to\infty} f(x, y) = \int_0^\pi f(x)\frac{du(x)}{dx}\frac{dx}{\pi}. \tag{3.36}$$

In view of (3.10) and (3.19), the singular integrals can be regularized as follows:

$$f(x) = f_\infty + \int_0^\pi \log|\cos u(x) - \cos u(x')|\,[f_{nsq}(x') - f_{nsq}(x)]\frac{dx'}{\pi} + f_{nsq}(x)(\hat{y}(x) - y_\infty - \log 2), \tag{3.37}$$

$$\frac{df(x)}{dx} = -\sin u(x)\int_0^\pi \frac{(du(x)/dx)\,f_{nsq}(x') - (du(x')/dx')\,f_{nsq}(x)}{\cos u(x) - \cos u(x')}\frac{dx'}{\pi}, \tag{3.38a}$$

$$f_{nsq}(x) = \int_0^\pi \frac{(du(x)/dx)\sin u(x')(df(x')/dx') - (du(x')/dx')\sin u(x)(df(x)/dx)}{\cos u(x) - \cos u(x')}\frac{dx'}{\pi}. \tag{3.38b}$$

These are the three basic equations for interrelating boundary values and derivatives of even-periodic harmonic functions. The logarithm and denominator coefficients are essentially the Green's function and Green's function normal derivative for this geometry. The complexity of the Green's function for the arbitrary bounding curve $y = \hat{y}(x)$ is encompassed by a single function $u(x)$ of one variable, which must be determined in a preliminary calculation. When $u(x)$ and du/dx are known, the above integrals may be calculated by interspersed Gaussian quadrature, as described in the next section.

IV. Numerical Solution of the Conformal Map Equations in Even-Periodic Geometry

In this section, an efficient numerical procedure is described for finding the boundary map function $u(x)$, and hence the entire conformal map.

1. *The Crowding Phenomenon*

As already noted, [1, 2] provide a variety of numerical conformal map procedures. They succeed by iterative and perturbation techniques when the boundary already approximates the one onto which it is to be mapped. When, however, the mapping requires a significant distortion of the original boundary, there is an underlying mathematical phenomenon to be confronted which we shall call "crowding." Its impact can be indicated by some numerical examples. Figure 1a shows the region R_z of the z plane with the lower boundary

$$y = \hat{y}(x) = -D \cos x \tag{4.1}$$

for the case $D = 5$. Figure 1b shows the region R_w from which it is conformally mapped and (4.1) is the image of $v = 0$. The grid of curves in R_z is the image under the mapping of the rectangular grid in R_w. For portions of R_z remote from $y = \hat{y}(x)$, the image mesh becomes approximately rectangular, and in fact,

$$x(u, v) \to u, \tag{4.2a}$$

$$y(u, v) \to v + y_\infty \tag{4.2b}$$

as $v \to \infty$ (and $y \to \infty$).

Near $y = \hat{y}(x)$, however, the grid geometry is dominated by the requirement that the images of $u =$ constant must be orthogonal to the boundary. This implies, as seen in Fig. 1a, that proceeding from $y = \hat{y}(x)$, the images of $u =$ constant on the left side of the boundary must veer left and are crowded against $x = 0$ before eventually straightening out and going vertical. It follows that in the correspondence of boundary points defined by $u = u(x)$, any interval Δx on the left side of the boundary of R_z will be crowded into a smaller interval Δu on the u-axis in R_w. Since the whole interval $0 \leqslant x \leqslant \pi$ is mapped onto the whole interval $0 \leqslant u \leqslant \pi$, there must be a compensating spreading of intervals Δx on the right side of R_z. We take $du(x)/dx$ as a numerical measure of this effect with $du/dx < 1$ signifying crowding and $du/dx > 1$ signifying inverse crowding i.e., spreading.

For curves of the class $\hat{y}(x) = -D \cos x$ with $D > 0$, maximum crowding is at $x = 0$ and maximum spreading is at $x = \pi$. Table III gives the values of du/dx at $x = 0$ and $x = \pi$ for $D = 1, 5, 10, 100$, as calculated by the techniques to be described in the next subsection. The magnitudes of crowding and spreading, as measured by du/dx, are seen to be of entirely different character for $D > 1$. The spreading in this class of examples increases slowly with D, while the crowding increases exponentially with D that is, du/dx goes down exponentially. If a numerical calculation of the map

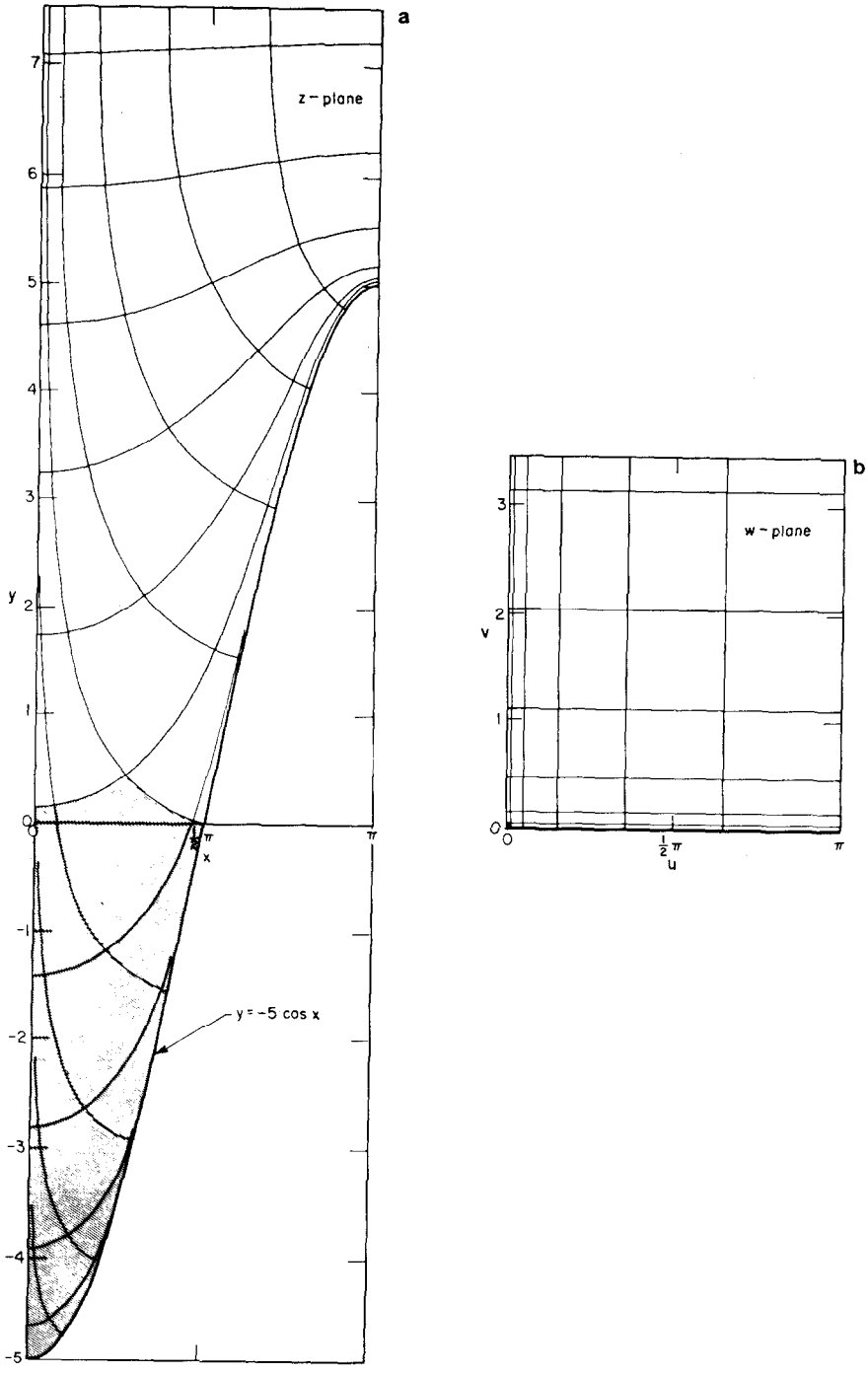

FIG. 1. The rectangular grid in region R_w of the w plane (b) is mapped into the grid of curves in region R_z of the z plane (a) under the conformal mapping $z = z(w)$ which carries the u-axis of the w plane into $y = -5 \cos x$. The small black square in the lower left corner of R_w is thereby mapped into the shaded region of R_z.

proceeds without recognition of the possibility of extreme crowding, there will be a danger of significant, or total, loss of accuracy, particularly with regard to the trough region of the boundary curve.

Suppose, for example, one seeks to map $v = 0$ onto $y = -10 \cos x$ by solving either of the two integral equations (3.21) or (3.22). Suppose, also, that one seeks to approximate the u-integral in either of these equations by a quadrature rule based on 100 equally spaced points in the interval of integration. Then, as may be inferred from Table I, *none* of these u-points, except $u = 0$, corresponds to the negative half of the $\hat{y}(x)$ curve. And for $D = 5$, *only one* such u-point corresponds to the negative half. The variation with x of the crowding is shown for this case by the logarithmic plot of du/dx in Fig. 2. In the trough region, the crowding is approximately exponential.

The equation for conformal mapping given most prominent attention in the literature is the Theodorsen–Garrick equation, which (see Section VIII.3) is essentially Eq. (3.21) in a different guise. This discussion of crowding points up the inadequacy of the Theodorsen–Garrick equation when applied to a highly distorted region, regardless of the technique of solution.

We shall turn, then, to the third integral equation, Eq. (3.23), where the natural variable of integration is x rather than u. This equation has the additional advantage that the logarithmic integrand is a smoother function than the integrands in Eqs. (3.21)

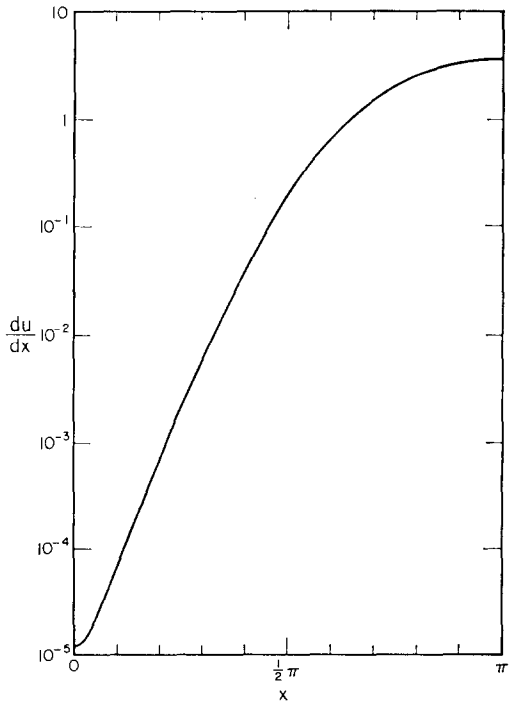

FIG. 2. The plot of du/dx for the case $y = -5 \cos x$ shows an approximately exponential variation of the crowding with x in the trough region.

and (3.22). As a result its integral can be better approximated by a quadrature rule. The question of how best to approximate the integral is discussed next.

2. *Gaussian Quadrature Methods*

Let the N solutions of the equation

$$\cos Nx = 0 \tag{4.3}$$

in the interval $0 \leqslant x \leqslant \pi$ be labeled x_i, $1 \leqslant i \leqslant N$ and let the $N + 1$ solutions of

$$\sin Nx = 0 \tag{4.4}$$

in this interval be labeled $\bar{x}_i$, $0 \leqslant i \leqslant N$. Thus

$$x_i = (i - \tfrac{1}{2})\pi/N, \qquad \bar{x}_i = i\pi/N. \tag{4.5}$$

Let $f(\cos x)$ be a function with at least $2N$ continuous derivatives with respect to $\cos x$. Then the Gauss–Chebyshev quadrature formula reads

$$\int_0^\pi f(\cos x)\frac{dx}{\pi} = \frac{1}{N}\sum_{i=1}^{N} f(\cos x_i) + E(N), \tag{4.6}$$

where the error term $E(N)$ can be estimated from

$$E(N) = \frac{2f^{(2N)}(\cos \xi)}{4^N(2N)!}, \qquad 0 < \xi < \pi.$$

For brevity, Eq. (4.6) without the error term will be called the C-rule of order $2N$. The C-rule is exact if $f(\cos x)$ is a polynomial in $\cos x$ of degree less than $2N$ or equivalently if $f(\cos x)$ represents a finite Fourier-cosine series terminating before the $\cos(2Nx)$ term. The x_i will be called C-points.

An alternative to (4.6) is the Gauss–Chebyshev–Lobatto formula, which reads

$$\int_0^\pi f(\cos x)\frac{dx}{\pi} = \frac{1}{N}\sum_{i=0}^{N} \epsilon_i f(\cos \bar{x}_i) - E(N), \tag{4.7}$$

where $\epsilon_i = \frac{1}{2}$ for $i = 0$ or $i = N$, and $\epsilon_i = 1$, otherwise. When the error term is dropped, this will be termed the L-rule of order $2N$ and the $\bar{x}_i$ will be called L-points. Equation (4.6) has the same form of error term as Eq. (4.6) but with opposite sign. This is consistent with the fact that the average of (4.6) and (4.7) produces an L-rule of order $4N$.

In some standard texts, equivalent rules are given in terms of $T_n(t)$ and $U_n(t)$, the Chebyshev polynomials of the first and second kind. The transition to trigonometric form is effected by setting $t = \cos x$ and

$$T_n(t) = \cos nx, \qquad U_n(t) = \sin nx/\sin x.$$

Now consider the application of these rules to an integral of the type

$$J(x) = \int_0^\pi \log \left| \frac{\cos u(x) - \cos u(x')}{\cos x - \cos x'} \right| \frac{dx'}{\pi} \tag{4.8}$$

which occurs in the third integral equation. Let $J_C(x)$ and $J_L(x)$ be the approximations by the C-rule and L-rule to $J(x)$. Let x_j be a C-point and $\bar{x}_j$ be an L-point. We have:

$$J_C(\bar{x}_j) = \frac{1}{N} \sum_{i=1}^{N} \log | \cos u(\bar{x}_j) - \cos u(x_i)| - I_C(\bar{x}_j), \tag{4.8a}$$

$$J_L(x_j) = \frac{1}{N} \sum_{i=0}^{N} \epsilon_i \log | \cos u(x_j) - \cos u(\bar{x}_i)| - I_L(x_j), \tag{4.8b}$$

where

$$I_C(\bar{x}_j) = \frac{1}{N} \sum_{i=1}^{N} \log | \cos \bar{x}_j - \cos x_i |, \tag{4.9a}$$

$$I_L(x_j) = \frac{1}{N} \sum_{i=0}^{N} \epsilon_i \log | \cos x_j - \cos \bar{x}_i |. \tag{4.9b}$$

The expressions for I_C and I_L can be simplified by using the identities

$$\prod_{i=1}^{N} (\cos x - \cos x_i) = 2^{-(N-1)} \cos Nx,$$

$$\prod_{i=1}^{N-1} (\cos x - \cos \bar{x}_i) = 2^{-(N-1)} \sin Nx / \sin x.$$

These hold because (a) in each case, both sides of the equation represent polynomials in $\cos x$ with the same zeros and (b) an analytic continuation of x into the complex z plane with $\operatorname{Im} z \to \infty$ yields the overall coefficient. Since the sum of logarithms is the logarithm of the product, we have

$$I_C(x) = -\log 2 + (1/N)\{\log 2 + \log | \cos Nx |\}, \tag{4.10a}$$

$$I_L(x) = -\log 2 + (1/N)\{\log 2 + \log | \sin Nx |\}. \tag{4.10b}$$

Inserting Eqs. (4.10) into Eqs. (4.8) we obtain

$$J_C(\bar{x}_j) = -\left(1 - \frac{1}{N}\right) \log 2 + \frac{1}{N} \sum_{i=1}^{N} \log | \cos u(\bar{x}_j) - \cos u(x_i)|, \tag{4.11a}$$

$$J_L(x_j) = -\left(1 - \frac{1}{N}\right) \log 2 + \frac{1}{N} \sum_{i=0}^{N} \epsilon_i \log | \cos u(x_j) - \cos u(\bar{x}_i)|. \tag{4.11b}$$

These rules are next applied to solve the third integral equation.

3. *Calculational Procedure*

We are given a function $\hat{y}(x)$ which is even periodic and single valued. We seek an unknown single-valued function $u(x)$ with $u(0) = 0$ and $u(\pi) = \pi$. The equation to be solved is

$$\hat{y}(x) = y_\infty + \int_0^\pi \log \left| \frac{\cos u(x) - \cos u(x')}{\cos x - \cos x'} \right| \frac{dx'}{\pi}. \tag{4.12}$$

We consider the sequences $\{x_i\}$, $\{\bar{x}_i\}$ as defined in (4.5). The two sequences interlace and taken together comprise $2N + 1$ points on the interval $0 \leqslant x \leqslant \pi$ including the end points $\bar{x}_0 = 0$, $\bar{x}_N = \pi$. Corresponding y and u sequences are specified by

$$y_i = \hat{y}(x_i), \qquad \bar{y}_i = \hat{y}(\bar{x}_i), \tag{4.13}$$

and

$$u_i = u(x_i), \qquad \bar{u}_i = u(\bar{x}_i). \tag{4.14}$$

Because $\bar{u}_0 = 0, \bar{u}_N = \pi$, a total of $2N - 1$ subscripted u's are unknown.

We now apply the C-rule to (4.12) to evaluate $\hat{y}(x)$ when x is an L-point and apply the L-rule for evaluation when x is a C-point. For $x = 0$, we have, by (4.11a),

$$\bar{y}_0 = y_\infty - \left(1 - \frac{1}{N}\right) \log 2 + \frac{1}{N} \sum_{i=1}^{N} \log | 1 - \cos u_i |, \tag{4.15}$$

which serves to express y_∞ in terms of the u's at C-points. Further, for $1 \leqslant j \leqslant N$,

$$y_j = y_\infty - \left(1 - \frac{1}{N}\right) \log 2 + \frac{1}{N} \sum_{i=0}^{N} \epsilon_i \log | \cos u_j - \cos \bar{u}_i |$$

so that

$$y_j - \bar{y}_0 - \frac{1}{N} \sum_{i=0}^{N} \epsilon_i \log | \cos u_j - \cos \bar{u}_i | + \frac{1}{N} \sum_{i=1}^{N} \log | 1 - \cos u_i | = 0$$

$$\text{for} \quad 1 \leqslant j \leqslant N. \tag{4.16}$$

Similarly,

$$\bar{y}_j - \bar{y}_0 - \frac{1}{N} \sum_{i=1}^{N} \{\log | \cos \bar{u}_j - \cos u_i | - \log | 1 - \cos u_i |\} = 0$$

$$\text{for} \quad 1 \leqslant j \leqslant N - 1. \tag{4.17}$$

Equations (4.16) and (4.17) constitute a set of $2N - 1$ nonlinear algebraic equations for $2N - 1$ unknowns which are the u_i, $1 \leqslant i \leqslant N$, and $\bar{u}_i$, $1 \leqslant i \leqslant N - 1$.

The integrand of (4.12) will have derivatives with respect to $\cos x'$ to the same order as $u(x')$ for $x \neq x'$, and to one order less for $x = x'$. Thus, for sufficiently smooth $u(x)$, the quadrature rules applied to (4.12) should have high accuracy for moderate values

of N. Because we have not sought to evaluate, say, $\hat{y}(x)$ at C-points by using the C-rule, we bypass the question of how to evaluate integrands at $x = x'$, that is, of how to calculate (du/dx) before we have determined $u(x)$. Note that we have taken the boundary conditions $u(0) = 0$ and $u(\pi) = \pi$ into account by using a closed quadrature rule (L-rule). Also, note that Eq. (4.17) has *the same form* that would result from naively applying the Gauss–Chebyshev quadrature rule to Eq. (3.19) with no concern for the logarithmic singularities. However, it is only valid when $\bar{x}_j$ is an L-point. This process of evaluating integrals by the C-rule to avoid calculating derivatives at L-points, and vice-versa, may be referred to as "interspersed Gaussian quadrature." It is equivalent to evaluating the integrand at $x = x'$ by interpolation based on a Fourier-cosine representation of $2N$ terms and then using the L-rule of order $4N$. The interpolation limits the accuracy to order $2N$.

Let $F_j(\mathbf{u}, \bar{\mathbf{u}})$ and $\bar{F}_j(\mathbf{u}, \bar{\mathbf{u}})$ denote, respectively, the left-hand sides of Eqs. (4.16) and (4.17), with the sets of variables $\{u_i\}$ and $\{\bar{u}_i\}$ denoted, respectively, by $\mathbf{u}$ and $\bar{\mathbf{u}}$. Then the system of equations to be solved for $\mathbf{u}$ and $\bar{\mathbf{u}}$ is

$$F_j(\mathbf{u}, \bar{\mathbf{u}}) = 0, \qquad 1 \leqslant j \leqslant N, \tag{4.18a}$$

and

$$\bar{F}_j(\mathbf{u}, \bar{\mathbf{u}}) = 0, \qquad 1 \leqslant j \leqslant N - 1. \tag{4.18b}$$

This is best done by a Newton–Raphson technique.

Suppose that $\mathbf{u}^{(n)}$ and $\bar{\mathbf{u}}^{(n)}$ represent the nth stage of an approximation to the solution to (4.18a), (4.18b). Let $\mathbf{u}$, $\bar{\mathbf{u}}$ denote the exact solution and let

$$\mathbf{u} = \mathbf{u}^{(n)} + \Delta\mathbf{u}, \qquad \bar{\mathbf{u}} = \bar{\mathbf{u}}^{(n)} + \Delta\bar{\mathbf{u}}$$

with $\Delta\mathbf{u}$ and $\Delta\bar{\mathbf{u}}$ presumed small.

Then, if second-order terms in $\Delta\mathbf{u}$, $\Delta\bar{\mathbf{u}}$ are dropped,

$$F_j + \sum_{k=1}^{N} \frac{\partial F_j}{\partial u_k} \Delta u_k + \sum_{m=1}^{N-1} \frac{\partial F_j}{\partial \bar{u}_m} \Delta \bar{u}_m = 0 \tag{4.19a}$$

and

$$\bar{F}_j + \sum_{k=1}^{N} \frac{\partial \bar{F}_j}{\partial u_k} \Delta u_k + \sum_{m=1}^{N-1} \frac{\partial \bar{F}_j}{\partial \bar{u}_m} \Delta \bar{u}_m = 0, \tag{4.19b}$$

where the F's and their partial derivatives are evaluated for $\mathbf{u}^{(n)}$, $\bar{\mathbf{u}}^{(n)}$. By (4.17),

$$\frac{\partial \bar{F}_j}{\partial \bar{u}_m} = 0 \qquad \text{if} \quad j \neq m. \tag{4.20}$$

Hence, from (4.19b)

$$\Delta \bar{u}_m = -\left(\bar{F}_m + \sum_{k=1}^{N} \frac{\partial \bar{F}_m}{\partial u_k} \Delta u_k\right) \Big/ (\partial \bar{F}_m / \partial \bar{u}_m). \tag{4.21}$$

Substituting (4.21) into (4.19a) we get

$$F_j - \sum_{m=1}^{N-1} \frac{\partial F_j}{\partial \bar{u}_m} \frac{\bar{F}_m}{(\partial \bar{F}_m / \partial \bar{u}_m)} + \sum_{k=1}^{N} Q_{jk} \Delta u_k = 0, \tag{4.22}$$

where the $N \times N$ matrix Q_{jk} is given by

$$Q_{jk} = \frac{\partial F_j}{\partial u_k} - \sum_{m=1}^{N-1} \frac{\partial F_j}{\partial \bar{u}_m} \frac{1}{(\partial \bar{F}_m / \partial \bar{u}_m)} \frac{\partial \bar{F}_m}{\partial u_k}. \tag{4.23}$$

The procedure is then the following: Given an approximate solution $\mathbf{u}^{(n)}$, $\bar{\mathbf{u}}^{(n)}$ of Eqs. (4.16), (4.17) one calculates the approximate correction $\Delta\mathbf{u}$ by solving the linear equation (4.22). Then $\Delta\bar{\mathbf{u}}$ is calculated from (4.21) and the next approximation to (4.16), (4.17) is given by

$$\mathbf{u}^{(n+1)} = \mathbf{u}^{(n)} + \Delta\mathbf{u}, \qquad \bar{\mathbf{u}}^{(n+1)} = \bar{\mathbf{u}}^{(n)} + \Delta\bar{\mathbf{u}}.$$

The approximation procedure is iterated until converge to the desired numerical accuracy is obtained. The problem of finding a reasonable initial approximation $\mathbf{u}^{(0)}$, $\bar{\mathbf{u}}^{(0)}$ to generate a sequence $\{\mathbf{u}^{(n)}, \bar{\mathbf{u}}^{(n)}\}$ which converges to the correct answer is not as hard as it looks; guidelines for this will be set forth in subsection (V.2). Then y_∞ can be calculated from (4.15).

The net result is to produce an evaluation of the function $u(x)$ at $2N + 1$ equally spaced data points on the interval $0 \leqslant x \leqslant \pi$. Each stage of the Newton–Raphson iteration requires inversion of an $N \times N$ matrix.

As is made plain by the formulas of (III.5), applications of the conformal map procedure may require knowledge of $du(x)/dx$ as well as $u(x)$. A feasible method, and perhaps the most accurate one in this scheme of calculation, is to go back to (4.12) and apply the C-rule when x is a C-point, and the L-rule when x is an L-point.

Specifically, the C-rule applied for $x = x_j$ yields

$$y_j = y_\infty + \frac{1}{N} \sum_{\substack{i=1 \\ i \neq j}}^{N} \log | \cos u_j - \cos u_i | + K_C(x_j), \tag{4.24a}$$

where

$$K_C(x_j) = \lim_{x \to x_j} \left[\frac{1}{N} \log \left| \frac{\cos u(x) - \cos u_j}{\cos x \quad \cos x_j} \right| + \frac{1}{N} \log | \cos x - \cos x_j | - I_C(x) \right]$$

$$= \log 2 + \frac{1}{N} \log \left| \frac{\sin u_j}{2N} \left(\frac{du}{dx} \right)_{x=x_j} \right|. \tag{4.24b}$$

Further, the L-rule applied for $x = \bar{x}_j$ yields

$$\bar{y}_j = y_\infty + \frac{1}{N} \sum_{\substack{i=0 \\ i \neq j}}^{N} \epsilon_i \log | \cos \bar{u}_j - \cos \bar{u}_i | + K_L(\bar{x}_j). \tag{4.25a}$$

For the cases $\bar{x}_j \neq 0$, $\bar{x}_j \neq \pi$, the calculation of K_L has the same form and the same result as for K_C :

$$K_L(\bar{x}_j) = \log 2 + \frac{1}{N} \log \left| \frac{\sin \bar{u}_j}{2N} \left(\frac{du}{dx}\right)_{x=\bar{x}_j} \right|. \tag{4.25b}$$

For $\bar{x}_j = 0$ or $\bar{x}_j = \pi$, $\sin \bar{u}_j = 0$ and

$$K_L(\bar{x}_j) = \lim_{x \to \bar{x}_j} \left[\frac{1}{2N} \log \left| \frac{\cos u(x) - \cos \bar{u}_j}{\cos x - \cos \bar{x}_j} \right| + \frac{1}{2N} \log |\cos x - \cos \bar{x}_j| - I_L(x) \right]$$

$$= \log 2 + \frac{1}{N} \log \left| \frac{1}{2N\, 2^{1/2}} \left(\frac{du}{dx}\right)_{x=\bar{x}_j} \right| \tag{4.25c}$$

Then (4.24) and (4.25) permit calculation of du/dx at the data points in terms of the already calculated values of y_∞ and $u(x)$ at these points, and provide a certain consistency between the C-rule and L-rule calculations. This method for calculating du/dx works well even when du/dx varies over many orders of magnitude due to the crowding phenomenon.

4. *Additional Calculational Considerations*

For the programming of the map calculation on a computer, the following points may be noted:

(a) In general, the sum of logarithms should be replaced by the logarithm of a product, so that the number of logarithms to be computed per Newton–Raphson step is of the order of $2N$ rather than $4N^2$. However, in cases of severe crowding and large N, the accumulated product of factors like $(\cos u_i - \cos u_j)$ can go off scale, i.e., become less than 10^{-300} and some adjustment of the product calculation should be made. Since most of the computer time is used to solve the linear equations, this is a small effect.

(b) The coordinates for the mapping problem should, if possible, be set up so that the crowding is in the neighborhood of $u = 0$, rather than $u = \pi$. This has been done in our numerical illustrations. Otherwise, a set of u-values may differ from π by very small amounts, complicating the task of preserving significant figures.

(c) When there is significant crowding of the u-data near $u = 0$, the calculation of $(\cos u_i - \cos u_j)$ by the difference of the cosines will lose significant figures. One remedy is to put

$$\cos u_i - \cos u_j = -2 \sin \tfrac{1}{2}(u_i - u_j) \sin \tfrac{1}{2}(u_i + u_j). \tag{4.26}$$

A simpler and usually adequate method is to rephase the formulas in terms of the versine function $\mathrm{ver}(u)$. Thus

$$\cos u_i - \cos u_j = \mathrm{ver}(u_j) - \mathrm{ver}(u_i), \tag{4.27}$$

where the versine is defined by ver $u = 1 - \cos u$ and calculated by

may overshoot resulting in output u-data which do not have these properties. In our calculations, when any output u-datum lay outside $(0, \pi)$, its value was redefind so that its distance from the nearest endpoint of the interval was adjusted to be a certain fraction $f, f < 1$, of its original distance, and the u-data were relabeled so as to make the $\mathbf{u}$ and $\bar{\mathbf{u}}$ series monotonic and interspersed. The "adjustment factor" might be $f = 10^{-1}$ or less depending on the anticipated crowding. This has no effect if the input u-data are a good approximation to the solution. But it greatly expands the range of initial data assumptions for which the iteration scheme converges.

(f) Some simple bounds can be placed on y_∞ in advance of the calculation. By Eq. (3.7) and the definition of y_∞, we have

$$y_\infty = \int_0^\pi y(u) \frac{du}{\pi} = \int_0^\pi \hat{y}(x(u)) \frac{du}{\pi}. \tag{4.29}$$

Let $y_{\min}$ and $y_{\max}$ be the minimum and maximum values assumed by $\hat{y}(x)$. Then

$$y_{\min} \leqslant y_\infty \leqslant y_{\max}. \tag{4.30}$$

Note also that for any u, u',

$$|\cos u - \cos u'| \leqslant 2$$

and so

$$\log |\cos u - \cos u'| \leqslant \log 2.$$

Then from Eq. (3.19)

$$\hat{y}(x) \leqslant y_\infty + 2 \log 2$$

for all $\hat{y}(x)$ and, in particular, for $y_{\max}$. This gives the more interesting bounds:

$$y_{\max} - 2 \log 2 \leqslant y_\infty \leqslant y_{\max}. \tag{4.31}$$

V. Numerical Examples

1. *Values of the Boundary Map Function $u(x)$ and Its Derivative*

Tables I and II display computed values of $u(x)$ and du/dx for 11 arguments as well as y_∞ for "cosine" curves

$$\hat{y}(x) = -D \cos x \tag{5.1}$$

and for "spike" curves

$$\hat{y}(x) = \frac{1}{2} D(1 + e^{\beta}) \left(1 - \frac{\sinh \beta}{\cosh \beta - \cos x}\right) \tag{5.2}$$

The spike curves are normalized so that

$$\hat{y}(\pi) = y_{\max} = D,$$

$$\hat{y}(0) = y_{\min} = -D \coth(\tfrac{1}{2}\beta),$$

and

$$\int_0^\pi \hat{y}(x) \frac{dx}{\pi} = 0.$$

[redacted]

Fig. 3.

The calculations followed the prescriptions of Section IV. In an Nth-order calculation, values of $u(x)$ and du/dx are found for $2N + 1$ equally spaced points x_k of which

TABLE

Boundary Map Function $u(x)$ and Its

	$D = 1$ $(N = 10)$		$D = 5$ $(N = 30)$	
x	$u(x)$	du/dx	$u(x)$	du/dx
0	0	0.2236 9558 9	0	$1.1627\ 7824 \times 10^{-5}$
0.1π	0.0734 0584 84	0.2536 2509 0	$8.6059\ 3926 \times 10^{-6}$	$6.7762\ 1730 \times 10^{-5}$
0.2π	0.1657 2663 9	0.3443 8025 9	$9.4166\ 8752 \times 10^{-5}$	$6.9554\ 0964 \times 10^{-4}$
0.3π	0.2962 4531 2	0.4966 2724 5	$8.7694\ 7213 \times 10^{-4}$	$5.9499\ 1440 \times 10^{-3}$
0.4π	0.4837 3523 7	0.7055 1678 5	$6.5574\ 6103 \times 10^{-3}$	0.0393 1682 93
0.5π	0.7439 4840 1	0.9561 9009 8	0.0373 8676 74	0.1894 6437 1
0.6π	1.0862 8577	1.2234 4491	0.1571 2708 8	0.6391 2105 5
0.7π	1.5111 1779	1.4759 6673	0.4828 6826 9	1.4941 2796
0.8π	2.0088 3315	1.6825 6048	1.1146 0230	2.5210 5348
0.9π	2.5607 7521	1.8175 9084	2.0413 4531	3.3106 3200
π	π	1.8644 9953	π	3.5991 3060
$y_\infty =$	0.4126 1222 3		4.0235 9218	

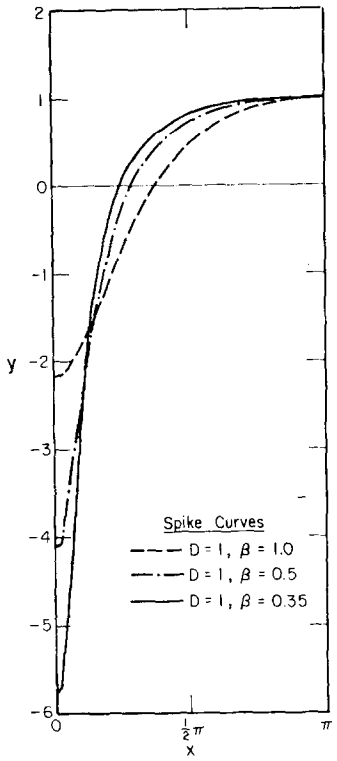

FIG. 3. These three spike curves define the lower boundaries of the regions R_z for which conformal map data are given in Tables II and IV.

I

Derivative for Cosine Curves (Eq. 5.1)

$D = 10$ $(N = 60)$		$D = 100$ $(N = 100)$	
$u(x)$	du/dx	$u(x)$	du/dx
0	$1.2099\ 5705 \times 10^{-11}$	0	2.8×10^{-121}
$5.2354\ 1694 \times 10^{-11}$	$8.0993\ 7164 \times 10^{-10}$	1.795×10^{-105}	2.8×10^{-103}
$6.0737\ 2218 \times 10^{-9}$	$8.9367\ 2965 \times 10^{-8}$	7.48×10^{-85}	1.1×10^{-82}
$5.1680\ 3585 \times 10^{-7}$	$6.9795\ 4847 \times 10^{-6}$	1.398×10^{-65}	1.95×10^{-63}
$2.8265\ 9276 \times 10^{-5}$	$3.3676\ 2934 \times 10^{-4}$	3.1118×10^{-48}	3.70×10^{-46}
$8.9369\ 8586 \times 10^{-4}$	$8.9668\ 0470 \times 10^{-3}$	2.8364×10^{-33}	2.84×10^{-31}
0.0151 6837 20	0.1209 4170 2	4.9731×10^{-21}	3.94×10^{-19}
0.1332 6193 4	0.7819 4771 1	$1.1166\ 43 \times 10^{-11}$	6.454×10^{-10}
0.6169 1984 7	2.4347 0375	$3.0666\ 3541 \times 10^{-5}$	$1.1270\ 634 \times 10^{-3}$
1.6755 4787	4.2012 0040	0.1399 9205 7	2.4161 7340
π	4.9038 0596	π	14.5616 970
	8.9140 7088		98.7148 079

TABLE II

Boundary Map Function $u(x)$ and Its Derivative for Spike Curves (Eq. 5.2)

	$D = 1, \beta = 1$ $(N = 50)$			$D = 1, \beta = 0.5$ $(N = 100)$			$D = 1, \beta = 0.35$ $(N = 100)$		
x	$\hat{y}(x)$	$u(x)$	du/dx	$\hat{y}(x)$	$u(x)$	du/dx	$\hat{y}(x)$	$u(x)$	du/dx
0	−2.16	0	$2.3114\,5931 \times 10^{-3}$	−4.08	0	3.773×10^{-10}	−5.77	0	1.4×10^{-19}
0.05π	−2.07	$5.9667\,3729 \times 10^{-4}$	$7.1288\,6627 \times 10^{-3}$	−3.61	$5.3793\,3 \times 10^{-8}$	2.9773×10^{-6}	−4.61	2.032×10^{-11}	2.552×10^{-9}
0.1π	−1.83	$3.2846\,6508 \times 10^{-3}$	0.0326 8320 46	−2.58	$6.1638\,381 \times 10^{-5}$	$2.1250\,38 \times 10^{-3}$	−2.69	$1.4383\,685 \times 10^{-5}$	$7.8571\,6 \times 10^{-4}$
0.15π	−1.49	0.0135 8620 49	0.1102 0331 7	−1.59	$3.7166\,1950 \times 10^{-3}$	0.0707 0949 47	−1.32	$4.2976\,7545 \times 10^{-3}$	0.0980 7682 42
0.2π	−1.12	0.0421 4807 55	0.2671 6801 5	−0.84	0.0351 0230 54	0.3685 7862 5	−0.50	0.0509 1244 40	0.5383 2599 4
0.25π	−0.75	0.1010 8636 6	0.4909 2812 1	−0.32	0.1251 6150 6	0.7729 6787 4	−0.01	0.1728 6799 2	0.9831 0540 1
0.3π	−0.43	0.1973 7157 5	0.7338 8429 7	0.05	0.2721 7612 8	1.0749 7658	0.30	0.3485 1148 1	1.2216 4970
0.4π	0.09	0.4938 1044 7	1.1226 2841	0.48	0.6584 9325 1	1.3246 1563	0.64	0.7585 5515 3	1.3417 9211
0.5π	0.44	0.8832 7011 2	1.3304 1790	0.71	1.0828 4640	1.3598 9620	0.80	1.1780 1341	1.3209 0268
0.75π	0.89	1.9971 1992	1.4552 8205	0.95	2.1306 1022	1.3043 6519	0.97	2.1807 1845	1.2404 1048
π	1.00	π	1.4568 3154	1.00	π	1.2786 4476	1.00	π	1.2151 4939
$y_\infty =$		0.5704 3808 7			0.6860 8057 2			0.7385 1920 3	

N are C-points and $N + 1$ are L-points. An initial approximation $\{u_k^{(0)}\} = \{u^{(0)}(x_k)\}$ is iterated by the Newton–Raphson method to yield a sequence $\{u_k^{(n)}\}$, $n = 1, 2, 3,...,$ until convergence to a desired accuracy level for the u_k and the $du(x_k)/dx$ is obtained for the Nth-order calculation. The main computing task at each Newton–Raphson step is the inversion of an $N \times N$ matrix. The calculation is repeated for a series of increasing values of N until the trend of data as a function of N converges to a desired accuracy.

The $D = 1$ case for the cosine curve is a comparative benign case. The first and second integral equations were also applied to this case and worked well, but not with such high accuracy for such low N values. The same appraisal probably would apply to the methods enumerated in Refs. [1, 2].

The cosine curves with $D = 5$, 10 and the spike curves with parameters as in Table II are typical of the boundary curves which motivated the present study of mapping techniques. They are characterized by severe crowding at the left end and even rough order-of-magnitude accuracy for mapping data on the crowded side poses a severe challenge to other currently known techniques.

The $D = 100$ cosine curve was included as a stunt to probe the limits of the third integral equation in conjunction with the prescribed interspersed quadrature technique.

2. *Choice of Initial Approximation and Convergence of the Newton–Raphson Iteration*

Following the nth step of the iteration, one can form an error estimate $E(n)$ by

$$E(n) = \operatorname*{Max}_k \left| \frac{u_k^{(n)} - u_k^{(n-1)}}{u_k^{(n)}} \right|. \tag{5.3}$$

If for some n, $E(n) < 0.1$, subsequent iterations in our experiments always converged quadratically; that is, the series $E(n + 1)$, $E(n + 2)$, etc., decreased at least as fast as the series 10^{-2}, 10^{-4}, etc. Thus, after three iterations following the $E(n) < 0.1$ level, the Nth-order problem (for N held fixed) is solved to the 14-figure accuracy of a modern computer for the values u_k. This behavior is, however, modified by accumulated round-off errors.

Let n_{NR} be the number of Newton–Raphson steps which, proceeding from the initial approximation, are done before reaching $E(n) < 0.1$. Then n_{NR} is primarily a measure of the quality of the initial approximation for $u(x)$. If the choice of the $u_k^{(0)}$ is sufficiently poor, the iteration may diverge.

We consider two alternatives for the initial approximation:

(A) *The "zero" approximation.* This refers to the simplest choice of input, namely,

$$u^{(0)}(x) = x \qquad \text{for all } x. \tag{5.4}$$

As a representative example, consider cosine curves and calculations of order $N = 30$, with an adjustment factor as defined in (IV.4.e) of $f = 10^{-5}$. Then the iteration process converges for all D at least up to $D = 100$. For $D = 1$, 5, 10, 100, we find $n_{NR} = 8$,

12, 17, and 24, respectively. If, instead, $f = 10^{-3}$, then for the same D-values, $n_{NR} = 6$, 8, 10, and 51, respectively. In general, $f = 10^{-5}$ is recommended for a first experiment; it leads to significantly faster convergence in extreme cases of crowding like $D = 100$, and to slightly slower convergence for smaller D-values.

The success of the trivial input assumption (5.4) is quite remarkable. For the $D = 100$ cosine curve, it means that 80% of the input u-values are wrong by from 5 to more than 100 orders of magnitude; yet the Newton–Raphson process converges to better than 10% relative accuracy for all u-values in as few as 25 iterations and converges to computer round-off accuracy in 3 additional iterations. This suggests that the combination of Newton–Raphson and adjustment procedures will suffice to solve the conformal map integral equation for a large class of boundary curves with little or no advance information about the character of the function $u(x)$ to be determined.

Now suppose that the zero approximation is adopted, but the adjustment process is not utilized. Then convergence is sensitive to whether y_∞ is eliminated by (4.15) or by the analogous equations for $\hat{y}(\pi)$, and the latter is better. Even so, the Newton–Raphson iteration will diverge for cosine curves with D of the order of one or more, the specific D-threshold for divergence depending on N. As a practical matter, the adjustment process or some equivalent to it is necessary for success of the method, except for cases of slight crowding.

(B) *The "shifted circle" approximation.* The number of needed Newton–Raphson iterations can be substantially reduced by a better choice for $u^{(0)}(x)$. Here, we define an elementary method for improvement based on the correspondence between periodic geometry and circular geometry. As noted in more detail in Section VIII, the mapping $W = -e^{-iw}$ carries the real w axis into the circumference of the unit circle $|W| = 1$ in the complex W plane. Similarly, periodic curves $y = \hat{y}(x)$ are mapped into certain closed curves in the complex Z plane, $Z = X + iY$, by $Z = -e^{-iz}$ and the original conformal map problem may be reformulated in terms of a mapping from the W to the Z plane.

Figure 4 portrays, roughly, the image curve in the Z plane for a curve $y = \hat{y}(x)$ in the z plane of the general type we have been studying. The curve has an oval shape in the large, but may have more complex shape in the immediate neighborhood of $X = 0$. Also shown in Fig. 4 is a circle drawn with the same horizontal diameter as the image of $y = \hat{y}(x)$. The circle has a radius R and is centered at $Z = X_0$, where

$$R = \tfrac{1}{2}(X_{\max} - X_{\min}) = \tfrac{1}{2}(e^{\hat{y}(\pi)} + e^{\hat{y}(0)}) \tag{5.5a}$$

and

$$X_0 = \tfrac{1}{2}(X_{\max} + X_{\min}) = \tfrac{1}{2}(e^{\hat{y}(\pi)} - e^{\hat{y}(0)}). \tag{5.5b}$$

The conformal map which carries the unit circle $|W| = 1$ onto the circle of Fig. 4 is

$$Z = RW + X_0 .$$

We now use this transformation, reexpressed in terms of the z and w planes, to define

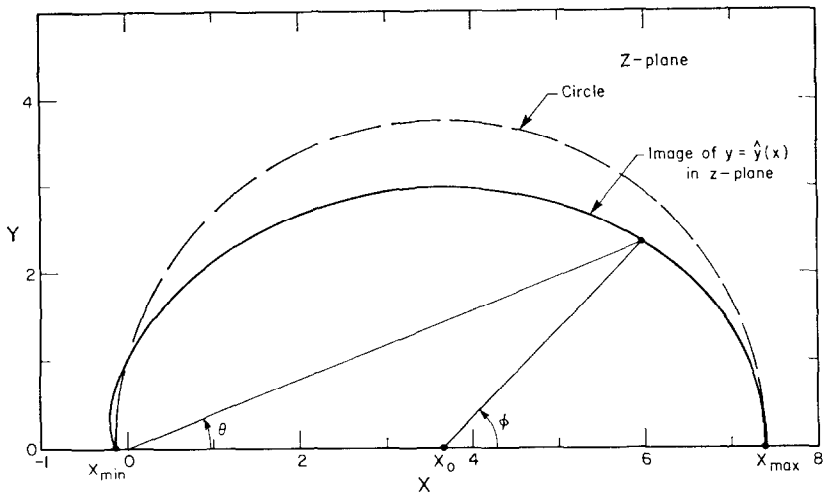

FIG. 4. The oval curve and superimposed circle in the Z-plane, $Z = -e^{-iz}$ provide the basis, for an initial approximation $u^{(0)}(x)$ for the boundary map function generated by a boundary in the z-plane. See Section V.2.

an initial approximation for $u = u(x)$. Given a point (X, Y) on the image curve in the Z plane, with θ and ϕ denoting the polar angles of this point in the Z and W planes, respectively, the geometry of Fig. 4 leads to

$$\cot \theta = \cot \phi - X_0/Y.$$

Making the identifications $\theta = \pi - x$, $\phi = \pi - u^{(0)}(x)$, $Y = e^{\hat{y}(x)} \sin x$, we infer the desired replacement for Eq. (5.4):

$$u^{(0)}(x) = \tan^{-1}\left(\frac{\sin x}{\cos x + e^{-\hat{y}(x)}X_0}\right). \tag{5.6}$$

Equation (5.6) with X_0 given by (5.5b) will be termed the shifted circle approximation.

The cases $D = 1$, 5, and 10 in Tables I and III were computed with the $u^{(0)}$ defined by Eq. (5.6) and an adjustment factor $f = 10^{-1}$. Use of a smaller f would increase the n_{NR}-values cited in Table III in these cases by one or two.

The remainder of the data in Tables I–IV were computed with $f = 10^{-5}$. For the lowest N-values cited for these cases, the shifted circle approximation was also used. Then for larger N-values, interpolations from the $u(x)$ calculated for the next lower N's were used to define the $u^{(0)}$, accelerating the Newton–Raphson converge somewhat. The resulting n_{NR}-values are listed in Tables III and IV. They are considerably smaller than those generated by the zero approximation.

TABLE III

Convergence of Boundary Map Function Derivatives for Cosine Curves with Increasing Order N of the Calculation[a]

	N	$(du/dx)_{x=0}$	$(du/dx)_{x=\pi}$	n_{NR}	Computer time (sec) per NR step (CDC-6600)
$D = 1$	15	0.2236 9558 9	1.8644 9953	0	0.09
	10	0.2236 9558 9	1.8644 9953	0	0.04
	5	0.2236 9564	1.8644 9953	0	0.01
	2	0.2244	1.8651	0	<0.003
$D = 5$	40	$1.1627\ 7824 \times 10^{-5}$	3.5991 3060	4	0.87
	30	$1.1627\ 7824 \times 10^{-5}$	3.5991 3060	4	0.43
	20	$1.1627\ 788 \times 10^{-5}$	3.5991 3060	4	0.16
	10	1.164×10^{-5}	3.5991 3060	4	0.04
	5	1.23×10^{-5}	3.5988	4	0.01
$D = 10$	60	$1.2099\ 5705 \times 10^{-11}$	4.9038 0596	5	3.03
	50	$1.2099\ 5706 \times 10^{-11}$	4.9038 0596	5	1.61
	40	$1.2099\ 576 \times 10^{-11}$	4.9038 0596	5	0.88
	30	$1.2099\ 8 \times 10^{-11}$	4.9038 0596	5	0.43
	20	1.211×10^{-11}	4.9038 0596	5	0.16
	10	1.29×10^{-11}	4.9038 03	5	0.04
$D = 100$	100	2.94×10^{-124}	14.5616 970	9	12.9
	80	3.23×10^{-124}	14.5616 970	10	6.62
	60	4.05×10^{-124}	14.5616 970	8	3.03
	40	7.5×10^{-124}	14.5616 971	8	0.89
	30	$15. \times 10^{-124}$	14.5616 8	9	0.43
	20	$75. \times 10^{-124}$	14.559	12	0.16

[a] See Section V.2 for definition of n_{NR} and initial approximation for $u(x)$.

3. *Convergence with Increasing N*

The accuracy of the computed $u(x)$ and du/dx must be inferred from the observed convergence trend in successive calculations with increasing N. The N-values listed in Tables I and II are sufficient to provide the data to the number of figures quoted and the approach to this level of accuracy is illustrated in Tables III and IV. We quote no more than nine significant figures in any case to avoid round-off error problems and the maximum N attempted was $N = 100$. In cases where $N = 100$ was not sufficient for nine-figure accuracy, the trend in convergence (which was geometric) for N increasing up to 100 was used for a conservative extrapolation of the last significant figure. (Compare the Table I datum for $(du/dx)_{x=0}$ at $D = 100$ and the trend in this datum in Table III.) In general du/dx converges less well with N than $u(x)$ and the worst case for convergence is at $x = 0$, where the crowding is greatest. Thus, the convergence of du/dx at $x = 0$ may be taken to indicate the minimum N needed to

TABLE IV

Convergence of Boundary Map Function Derivatives for Spike Curves with Increasing Order N[a]

	N	$(du/dx)_{x=0}$	$(du/dx)_{x=\pi}$	n_{NR}
$D = 1$,	50	$2.3114\,5931 \times 10^{-3}$	1.4568 3154	3
$\beta = 1$	40	$2.3114\,5933 \times 10^{-3}$	1.4568 3154	2
	30	$2.3114\,61 \times 10^{-3}$	1.4568 3154	3
	20	2.3117×10^{-3}	1.4568 3154	2
	10	2.35×10^{-3}	1.4568 36	8
$D = 1$,	100	3.7745×10^{-10}	1.2786 4476	9
$\beta = 0.5$	80	3.79×10^{-10}	1.2786 4476	8
	60	3.82×10^{-10}	1.2786 4476	8
	40	4.1×10^{-10}	1.2786 4476	8
	20	6.7×10^{-10}	1.2786 6	8
$D = 1$,	100	1.51×10^{-19}	1.2151 4939	12
$\beta = 0.35$	80	1.70×10^{-19}	1.2151 4939	10
	60	2.2×10^{-19}	1.2151 4939	8
	40	4.1×10^{-19}	1.2151 4940	8
	30	8.3×10^{-19}	1.2151 6	9
	20	$35. \times 10^{-19}$	1.219	8

[a] See Section V.2 for definition of n_{NR} and initial approximation for $u(x)$. Computation times are sensitive only to N and are like those in Table III.

ensure a definite level of relative accuracy for the data overall. The trend of du/dx values at $x = \pi$ is illustrative of convergence rates for data in the uncrowded region, which is always much faster than the rate in the crowded region.

Equations (3.37), Eq. (3.38a), and Eq. (3.38b) exemplify the principal intended application of our map techniques to boundary-value problems for harmonic functions. They show that, in general, du/dx data are needed as well as $u(x)$ data. If, for a case of severe crowding, accurate harmonic function data are needed near the trough region, then accurate values of $u(x)$ and du/dx are also needed in this region because, although very small, they multiply logarithms or denominators in the integrals which can be compensatingly large.

Suppose, however, that one deals with a class of problems where accurate harmonic function data are only required at the uncrowded end of the boundary or in the interior of the region not near to the trough of the boundary curve. Then, for a case of severe crowding, the very small values of $u(x)$ and du/dx at the trough end may be approximated by zero. For such problems a sufficient (and much lower) estimate of the required N is given by the observed convergence of du/dx at $x = \pi$, i.e., the uncrowded end.

4. *Interpolation for Intermediate x-Values*

The numerical procedure we have described computes $u(x)$ and du/dx only at equally spaced x points. The values of $u(x)$ at additional points may be obtained by

interpolation. Due to crowding du/dx may vary over many orders of magnitude. As a result, rather than interpolate $u(x)$ directly, it is better to interpolate a slowly varying function of u. A suitable function is

$$g(\cos x) = \log\left(\frac{\sin u(x)}{\sin x}\right).$$

At the endpoints,

$$g(1) = \log\left(\frac{du}{dx}\right)_{x=0} \qquad \text{and} \qquad g(-1) = \log\left(\frac{du}{dx}\right)_{x=\pi}.$$

By interpolating the function based on $\cos x$ as the independent variable, additional values of $u(x)$ may be obtained.

An alternate approach would be to go back to the original quadrature rules for approximating the third integral equation. We shall discuss this mainly to point out a certain pitfall. Suppose we approximate Eq. (3.23) by evaluating the integral with the C-rule of order $2N$ for arbitrary x. We get

$$\hat{y}(x) = y_\infty + \frac{1}{N}\sum_i \{\log|\cos u(x) - \cos u_i| - \log|\cos x - \cos x_i|\}$$

$$= y_\infty + \left(1 - \frac{1}{N}\right)\log 2 - \frac{1}{N}\log|\cos Nx| + \frac{1}{N}\sum_i \log|\cos u(x) - \cos u_i|.$$

(The summations over i refer only to those x_i which are C-points.) This can be rewritten in the form

$$L(x) = R(u), \tag{5.7}$$

where

$$L(x) = \left(\tfrac{1}{2}\right)^{(1-1/N)}|\cos Nx|^{1/N} e^{\hat{y}(x)-y_\infty}, \tag{5.8}$$

$$R(u) = \left\{\prod_i |\cos u - \cos u_i|\right\}^{1/N}. \tag{5.9}$$

The function $R(u)$ has N zeros, one for each $u = u_i$. In order for (5.7) to have a monotonically increasing solution $u(x)$ the function $L(x)$ must have zeros only at the N points $x = x_i$ and the extrema of $L(x)$ and $R(u)$ must correspond. In this case, between successive minima and maxima, (5.7) has a unique solution which can be used to assign values to $u(x)$. In general, extrema of the $L(x)$ and $R(u)$ will differ by some small amount of the order of the error in the overall calculation. Therefore, (5.7) will fail to have a well-defined solution near the extrema.

Mitchell Feigenbaum of Los Alamos has found an alternative approach which avoids this difficulty. He would choose a set of x_i which are C-points and apply the C-rule to evaluate the integral at a set of points x_m which are precisely the extrema of

$L(x)$ given by (5.8). The unknowns are the sets of $u_i = u(x_i)$ and $u_m = u(x_m)$. The sets of equations determining them are

$$L(x_m) = R(u_m), \qquad 0 = (dR/du)_{u=u_m}.$$

Then the calculation produces an exact match at the extrema of $L(x)$ and $R(u)$. The method fails if $L(x)$ has more than one extremum between adjacent quadrature points; this can be avoided by making N, the order of the rule, large enough. The details of this method will be described elsewhere by Feigenbaum.

Feigenbaum's method requires an analytic representation of $\hat{y}(x)$ in order to determine where the derivatives of $L(x)$, as given by (5.8), vanish. The method seems inappropriate if $\hat{y}(x)$ is specified by a finite number of data points, for some interpolation scheme will then be needed to evaluate the zeros of dL/dx; this would probably be the source of largest error in the calculation.

5. *Calculation of the Map in the Interior of the Regions*

Expressions for an analytic function $F(w)$ in the interior of R in terms of boundary values are given by (3.6a) and (3.6b). With the replacements of Eqs. (3.13), we get

$$z = w + \sin w \int_0^\pi \frac{y(u')}{\cos w - \cos u'} \frac{du'}{\pi}$$

and

$$-iz = y_\infty - iw - \int_0^\pi \frac{\sin u'[x(u') - u']}{\cos w - \cos u'} \frac{du'}{\pi}.$$

Integrating by parts and applying (3.11a), we also have

$$\begin{aligned} -iz &= y_\infty - iw + \int_0^\pi \log(\cos w - \cos u') \left(\frac{dx'}{\pi} - \frac{du'}{\pi}\right) \\ &= y_\infty + \log 2 + \int_0^\pi \log(\cos w - \cos u(x')) \frac{dx'}{\pi}. \end{aligned}$$

For the calculation of $z = z(w)$ when $v = \mathrm{Im}(w)$ is large, any of the above formulas, approximated by, e.g., a C-rule or an L-rule, is serviceable. But for $v \to 0$, the imaginary parts of the integrands vary sharply within a small interval and are best avoided. Taking the real parts only, we have these alternatives (among others):

$$x(u, v) = u + \mathrm{Re}\left[\sin w \int_0^\pi \frac{y(u')}{\cos w - \cos u'} \frac{du'}{\pi}\right], \tag{5.10}$$

$$y(u, v) = y_\infty + v - \mathrm{Re}\left[\int_0^\pi \frac{\sin u'[x(u') - u']}{\cos w - \cos u'} \frac{du'}{\pi}\right]. \tag{5.11}$$

Setting $F(w) = 1$ in Eq. (3.6a), we find

$$\mathrm{Re}\left[\int_0^\pi \frac{\sin w}{\cos w - \cos u'}\,\frac{du'}{\pi}\right] = 0.$$

This permits a subtraction in the integrands of (5.10), (5.11) to make the integrals more regular for $v \to 0$:

$$x(u, v) = u + \mathrm{Re}\left[\sin w \int_0^\pi \frac{\hat{y}(x') - \hat{y}(x(u))}{\cos w - \cos u'}\,\frac{du(x')}{dx'}\,\frac{dx'}{\pi}\right], \tag{5.12}$$

$$y(u, v) = y_\infty + v - \mathrm{Re}\left[\int_0^\pi \frac{\sin u(x')[x' - u(x')] - \sin w[x(u) - u]}{\cos w - \cos u'}\,\frac{du(x')}{dx'}\,\frac{dx'}{\pi}\right]. \tag{5.13}$$

Once $u(x)$ and du/dx are determined at sufficiently many data points along $y = \hat{y}(x)$, Eqs. (5.12) and (5.13) suffice to determine the mapping from the interior of R_w to the interior of R_z.

As an application, consider Fig. 1, which illustrates the map induced by $y = -5 \cos x$ in terms of a rectangular grid in the w plane and the image grid of curves in the z plane. First, a set of equally spaced abscissas $x_k = k\pi/10$, $0 \leqslant k \leqslant 10$ was selected and the corresponding u_k determined by a map calculation. These are precisely the u_k listed in the $D = 5$ column of Table I. For the drawing of Fig. 1, a calculation of order $N = 10$ is sufficient. Then the x_k are L-points and (5.12), (5.13) are to be approximated by the C-rule. The w-plane grid in Fig. 1b consists of the lines $u = u_k$, $v = u_k$, $0 \leqslant k \leqslant 10$. Because some u_k are very small, not all the rectangular grid lines are separately distinguishable in the figure. The image curves of this grid in Fig. 1a are

[redacted]

the shaded region of R_z in Fig. 1a, which occupies the whole of R_z below the x-axis, is the map of a nearly invisible square in the lower left corner of R_w; the side of this square has length 0.037. Also, note how rapidly the image curve of $v =$ constant flattens out above $\hat{y}_{\max}$.

VI. A Differential Approach

Suppose the z-plane boundary curve depends continuously on a parameter t, that is, $y = \hat{y}(x, t)$. Then the conformal map transformation generalizes to

$$z = z(w, t). \tag{6.1}$$

The boundary map function, its inverse, and the constant in the third integral equation will be denoted by $u(x; t)$, $x(u; t)$, and $y_\infty(t)$, respectively.

The main purpose of this section is to derive the formula

$$u_t(x;t) = \sin u(x;t) \int_0^\pi \frac{(u_x(x';t))^2}{1+(\hat{y}_x(x',t))^2} \frac{\hat{y}_t(x,t)-\hat{y}_t(x',t)}{\cos u(x;t)-\cos u(x';t)} \frac{dx'}{\pi}, \quad (6.2)$$

where partial differentiation with respect to x and t is indicated by subscripts.

This formulation may be useful for a potential problem with a moving boundary. Let t represent the time variable. If $\hat{y}(x,t)$ is either specified in advance, or determinable together with $\hat{y}_t(x,t)$ from other data at time t, then (6.2) provides a time differential equation for $u(x;t)$. Integration of (6.2) is an alternative to mapping calculations, as prescribed in Section IV, which otherwise have to be repeated at each time step in a dynamical calculation.

An additional consideration is noteworthy when the boundary motion as defined by $y = \hat{y}(x,t)$ is not specified beforehand, but is to be determined concurrently with other dynamical data. From (4.29), we have

$$y_\infty(t) = \int_0^\pi \hat{y}(x,t)\, u_x(x;t) \frac{dx}{\pi}.$$

Differentiating with respect to t and integrating by parts in one of the resulting terms, we get

$$dy_\infty(t)/dt = \int_0^\pi [\hat{y}_t(x,t)\, u_x(x;t) - \hat{y}_x(x,t)\, u_t(x;t)] \frac{dx}{\pi}. \quad (6.3)$$

Now when $u(x;t)$ and $y_\infty(t)$ are known, $\hat{y}(x,t)$ is determined from (3.23) and $u_x(x,t)$ from (4.24) and (4.25), all by quadratures. Thus, integration of (6.2) together with (6.3) represents a *substitute* for the task of integrating time differential equations for $\hat{y}(x,t)$, rather than an *additional* task.

To verify (6.2), we first ask how $u_t(x;t)$ can be related to the boundary value of an even-periodic function analytic in R_w, so that the integral relations connecting the real and imaginary parts of such boundary values [illegible] (3.12)

have

$$z(w,t) = w + iF(w,t)$$

where $F(w,t)$ is an even-periodic function and analytic in R_w. Then $dz(w,t)/dw$ and $iz_t(w,t)$ are likewise even-periodic. On the lower boundary of R_w, i.e., for $v = 0$, (6.1) becomes

$$x + i\hat{y}(x,t) = z(u,t). \quad (6.4)$$

It is understood that in boundary equations such as (6.4), the variables x and u are related by $u = u(x;t)$. Then differentiation of (6.4) with respect to t, holding x constant, yields

$$i\hat{y}_t(x,t) = \left(\frac{dz(w,t)}{dw}\right)_{v=0} u_t(x;t) + z_t(u,t).$$

Furthermore,

$$\left(\frac{dz(w,\,t)}{dw}\right)_{v=0} = \frac{dx(u;\,t)}{du} + i\,\frac{d\hat{y}(x(u;\,t),\,t)}{du}$$

$$= [1 + i\hat{y}_x(x,\,t)]/u_x(x;\,t).$$

It is now expedient to define a function $G(w)$ by

$$G(w) = -iz_t(w,\,t)(dz(w,\,t)/dw)^{-1}.$$

Then $G(w)$ is even-periodic and analytic in R_w. Moreover,

$$(G(w))_{v=0} = \frac{u_x(x;\,t)\,\hat{y}_t(x,\,t)}{1 + i\hat{y}_x(x,\,t)} + iu_t(x;\,t).$$

Thus, $u_t(x;\,t)$ enters into the imaginary part of $G(w)$ on the boundary, but not into the real part. We now apply Eq. (3.8a) to $G_R(u,\,0)$ and $G_I(u,\,0)$. After a change of integration variable by

$$du' = u_x(x';\,t)\,dx',$$

the result is

$$u_t(x;\,t) = \frac{u_x(x;\,t)\,\hat{y}_x(x,\,t)}{1 + (\hat{y}_x(x,\,t))^2}\,\hat{y}_t(x,\,t) - \sin u(x;\,t)$$

$$\times \text{ p.v.} \int_0^\pi \frac{(u_x(x';\,t))^2}{1 + (\hat{y}_x(x',\,t))^2}\,\frac{y_t(x',\,t)}{\cos u(x;\,t) - \cos u(x';\,t)}\,\frac{dx'}{\pi}. \tag{6.5}$$

The coefficient of $\hat{y}_t(x,\,t)$ in (6.5) is the negative imaginary part of $(dz/dw)^{-1}$ at $v = 0$. Since $(dz/dw)^{-1}$ is also even-periodic and analytic, this coefficient can be replaced by an integral over the real part of $(dz/dw)^{-1}$ at $v = 0$ by again applying Eq. (3.8a). When this is done, the result is Eq. (6.2), which was to be proved. For numerical purposes, (6.2) is preferable to (6.5) because the integral in (6.2) is nonsingular and can be evaluated by interspersed Gaussian quadrature.

As an alternative to variation through a parameter t, one may consider general functional variations:

$$\hat{y}(x) \to \hat{y}(x) + \delta\hat{y}(x), \qquad u(x) \to u(x) + \delta u(x).$$

Then the content of (6.5) can be reexpressed in terms of functional derivatives:

$$\frac{\delta u(x)}{\delta\hat{y}(x')} = \frac{u_x(x')}{1 + (\hat{y}_x(x'))^2}\left[\hat{y}_x(x')\,\delta(x - x') - \frac{\text{p.v.}}{\pi}\,\frac{u_x(x')\sin u(x)}{\cos u(x) - \cos u(x')}\right]. \tag{6.6}$$

PART B

VII. Periodic Geometry

In this section and the next two, the main formulas and methods developed for the even-periodic case are extended to related geometries. In addition to providing a greater degree of completeness, this allows a more direct comparison of our methods with those developed for airfoils. Moreover, certain analytic and approximate techniques for the periodic situations appear more clearly and better motivated when viewed in the circle geometry.

1. *Representations in Terms of Boundary Values*

Let $F(w)$ be a periodic analytic function in the upper-half w plane, but not necessarily even, and such that

$$F(w) \to F(\infty) + O(1/|w|) \qquad \text{as } |w| \to \infty.$$

Then we redefine the region R_w to comprise the upper-half strip $-\pi \leqslant u \leqslant \pi, 0 \leqslant v < \infty$. For w in the interior of R_w, Eqs. (3.1a) and (3.3a) are valid. If the integration contours in these equations are extended to the boundaries of R_w, then

$$F(w) = -i \sin w \int_{-\pi}^{\pi} \frac{F(u')}{\cos w - \cos u'} \frac{du'}{2\pi} \tag{7.1}$$

and

$$F(w) = F(\infty) - i \int_{-\pi}^{\pi} \frac{\sin u' \, F(u')}{\cos w - \cos u'} \frac{du'}{2\pi}. \tag{7.2}$$

because the integrals over the vertical boundaries $u = -\pi$ and $u = \pi$ cancel by periodicity. From (7.1), we infer

$$F(\infty) = \int_{-\pi}^{\pi} F(u') \frac{du'}{2\pi}. \tag{7.3}$$

Next, let $w \to u$ from the interior of R_w and note that for u and u' restricted to the interval $(-\pi, \pi)$, $(\cos u - \cos u')$ has zeros for $u' = u$ and $u' = -u$. The generalizations of (3.4) for this interval are

$$\lim_{w \to u} \frac{\sin w}{\cos w - \cos u'} = \text{p.v.} \frac{\sin u}{\cos u - \cos u'} + \pi i[\delta(u - u') + \delta(u + u')] \tag{7.4a}$$

and

$$\lim_{w \to u} \frac{\sin u'}{\cos w - \cos w'} = \text{p.v.} \frac{\sin u'}{\cos u - \cos u'} + \pi i[\delta(u - u') - \delta(u + u')]. \tag{7.4b}$$

The useful combination of (7.4a) and (7.4b) is the one that cancels the $\delta(u + u')$ term. Noting the trigonometric identity

$$\frac{\sin w + \sin u'}{\cos w - \cos u'} = -\cot\frac{1}{2}(w - u'), \tag{7.5}$$

we average (7.1) and (7.2) to get

$$F(w) = \frac{1}{2}F(\infty) + \frac{i}{2}\int_{-\pi}^{\pi}\cot\frac{1}{2}(w - u')\,F(u')\,\frac{du'}{2\pi}. \tag{7.6a}$$

For w interior to R_w, w^* is outside, and so the same process yields

$$0 = \frac{1}{2}F(\infty) + \frac{i}{2}\int_{-\pi}^{\pi}\cot\frac{1}{2}(w^* - u')\,F(u')\,\frac{du'}{2\pi}. \tag{7.6b}$$

Thus, taking the sum and difference of (7.6a) with the complex conjugate of (7.6b), we have the two alternatives:

$$F(w) = F_R(\infty) - \int_{-\pi}^{\pi}\cot\frac{1}{2}(w - u')\,F_I(u', 0)\,\frac{du'}{2\pi}, \tag{7.7a}$$

$$F(w) = iF_I(\infty) + i\int_{-\pi}^{\pi}\cot\frac{1}{2}(w - u')\,F_R(u', 0)\,\frac{du'}{2\pi}. \tag{7.7b}$$

Adding (7.4a) and (7.4b), we get

$$\lim_{w\to u}\cot\tfrac{1}{2}(w - u') = \text{p.v. }\cot\tfrac{1}{2}(u - u') - 2\pi i\,\delta(u - u'). \tag{7.7}$$

Hence, taking the limit $w \to u$ in (7.7a) and (7.7b) we get

$$F_R(u, 0) = F_R(\infty) - \text{p.v.}\int_{-\pi}^{\pi}\cot\frac{1}{2}(u - u')\,F_I(u', 0)\,\frac{du'}{2\pi} \tag{7.8a}$$

and

$$F_I(u, 0) = F_I(\infty) + \text{p.v.}\int_{-\pi}^{\pi}\cot\frac{1}{2}(u - u')\,F_R(u', 0)\,\frac{du'}{2\pi}. \tag{7.8b}$$

Adding (3.5a) and (3.5b), we have

$$-2\frac{d}{du'}\log\left|\sin\frac{1}{2}(u - u')\right| = \cot\frac{1}{2}(u - u'). \tag{7.9}$$

Thus, integration by parts yields

$$F_R(u, 0) = F_R(\infty) - 2\int_{-\pi}^{\pi}\log\left|\sin\frac{1}{2}(u - u')\right|\frac{dF_I(u', 0)}{du'}\,\frac{du'}{2\pi} \tag{7.10}$$

and a similar representation for $F_I(u, 0)$. The endpoint terms cancel because $F_R(u, 0)$ and $F_I(u, 0)$ are periodic.

In the case where $F(w)$ is even as well as periodic, these formulas reduce to those of Section III. Conversely, any periodic $F(w)$ can be written as

$$F(w) = F_1(w) + iF_2(w), \tag{7.11}$$

where $F_1(w)$ and $F_2(w)$ are even periodic. Then introduction of the representations of Section III for $F_1(w)$ and $F_2(w)$ in (7.11) leads to an alternative derivation of the formulas of the present section. The definitions of these even periodic functions are

$$F_1(w) = [F(w) + F^*(-w^*)]/2, \tag{7.12a}$$

$$F_2(w) = [F(w) - F^*(-w^*)]/(2i). \tag{7.12b}$$

2. *Integral Equations for Conformal Mapping*

In analogy to the method and notation of Section III.4, we consider a curve $y = \hat{y}(x)$ in the z plane where $\hat{y}(x + 2\pi) = \hat{y}(x)$. Let

$$z = z(w) = w + iF(w) \tag{7.13}$$

be a conformal mapping of the upper-half w plane onto the z-region above $y = \hat{y}(x)$ which carries $w = i\infty$ into $z = i\infty$. Again we have

$$x(u, v) = u - F_I(u, v), \qquad y(u, v) = v + F_R(u, v), \tag{7.14}$$

and $x(u)$, $y(u)$ defined by

$$x(u) \equiv x(u, 0) = u - F_I(u, 0), \qquad y(u) \equiv y(u, 0) = F_R(u, 0). \tag{7.15}$$

And also, $y(u) = \hat{y}(x(u))$.

The periodicity of F_I implies

$$x(\pi) - x(-\pi) = 2\pi. \tag{7.16}$$

Since addition of an imaginary constant to $F(w)$ does not alter the nature of the map, we are at liberty to specify

$$x(\pi) = \pi, \qquad x(-\pi) = -\pi. \tag{7.17}$$

In the limit $v \to \infty$, we have

$$x(u, v) \to u + x_\infty, \qquad y(u, v) \to + y_\infty, \tag{7.18}$$

where x_∞ and y_∞ are identified with $-F_I(\infty)$, $F_R(\infty)$, respectively.

Then Eqs. (7.8) convert into

$$x(u) = u + x_\infty - \text{p.v.} \int_{-\pi}^{\pi} \cot \frac{1}{2}(u - u')\, y(u') \frac{du'}{2\pi} \tag{7.19a}$$

and

$$y(u) = y_\infty + \text{p.v.} \int_{-\pi}^{\pi} \cot \frac{1}{2}(u - u')[x(u') - u'] \frac{du'}{2\pi}. \tag{7.19b}$$

These are the analogs of the first and second integral equations for the mapping problem derived in Section III. To obtain the analog of the third integral equation, we first evaluate the integral

$$I(u) = \int_{-\pi}^{\pi} \log \left| \sin \frac{1}{2}(u - u') \right| \frac{du'}{2\pi}.$$

We have

$$\begin{aligned} I(u) &= \frac{1}{2} \int_{-\pi}^{\pi} \log \left| \frac{1 - \cos(u - u')}{2} \right| \frac{du'}{2\pi} \\ &= \frac{1}{2} \int_{-\pi}^{\pi} (\log | 1 - \cos u' | - \log 2) \frac{du'}{2\pi} \\ &= -\log 2, \qquad \text{independent of } u. \end{aligned} \tag{7.20}$$

Thus, by (7.10) and (7.14),

$$\hat{y}(x) = y_\infty + 2 \log 2 + 2 \int_{-\pi}^{\pi} \log \left| \sin \frac{1}{2}(u(x) - u(x')) \right| \frac{dx'}{2\pi}. \tag{7.21}$$

Setting $F(w) = 1$ in (7.8b), we infer

$$\text{p.v.} \int_{-\pi}^{\pi} \cot \frac{1}{2}(u - u') \frac{du'}{2\pi} = 0. \tag{7.22}$$

With this and (7.18), the three integral equations can be expressed in nonsingular form as

$$x(u) = u + x_\infty - \int_{-\pi}^{\pi} \cot \frac{1}{2}(u - u')[y(u') - y(u)] \frac{du'}{2\pi}, \tag{7.23a}$$

$$y(u) = y_\infty + \int_{-\pi}^{\pi} \cot \frac{1}{2}(u - u')[(x(u') - u') - (x(u) - u)] \frac{du'}{2\pi}, \tag{7.23b}$$

$$\hat{y}(x) = y_\infty + 2 \int_{-\pi}^{\pi} \log \left| \frac{\sin \frac{1}{2}(u(x) - u(x'))}{\sin \frac{1}{2}(x - x')} \right| \frac{dx'}{2\pi}. \tag{7.23c}$$

The term x_∞ in (7.23a) can be removed by setting $x(u) \to x(u) + x_\infty$; this amounts to an adjustment of $x(u, v)$ at the cost of giving up the specifications (7.17).

3. *The Theodorsen Form*

The singularities of (7.19) can be removed in another way. Since both $\cot \frac{1}{2}(u - u')$, and $y(u')$ are of period 2π in u', we can translate the integrals to get

$$\text{p.v.} \int_{-\pi}^{\pi} \cot \frac{1}{2}(u - u')\, y(u')\, du' = -\,\text{p.v.} \int_{-\pi}^{\pi} \cot \left(\frac{1}{2} u'\right) y(u + u')\, du',$$

which shifts the singularities to the fixed point $u' = 0$. If we then apply the rule

$$\int_{-\pi}^{\pi} f(t) \frac{dt}{2\pi} = \int_{0}^{\pi} \frac{f(t) + f(-t)}{2} \frac{dt}{\pi}, \tag{7.24}$$

Eqs. (7.19) become

$$x(u) = u + x_\infty - \frac{1}{2} \int_0^{\pi} \cot \left(\frac{1}{2} u'\right) [y(u - u') - y(u + u')] \frac{du'}{\pi}, \tag{7.25a}$$

$$y(u) = y_\infty + \frac{1}{2} \int_0^{\pi} \cot \left(\frac{1}{2} u'\right) [x(u - u') - x(u + u') + 2u'] \frac{du'}{\pi}. \tag{7.25b}$$

Apart from the dispensable constant x_∞, these are substantially the Theodorsen–Garrick forms of the conformal mapping equations, or at least will be if the appropriate transition is made to the more familiar case of circle geometry (see next section).

4. *Numerical Procedures*

To apply our Gaussian quadrature methods to the solution of the family of integral equations (7.23), we first apply the rule (7.24). If this is done to (7.23a) after replacing the cotangent via (7.5), the result is

$$x(u) = u + x_\infty + \frac{1}{2} \int_0^{\pi} \frac{\sin u[y(u') + y(-u') - 2y(u)] + \sin u'[y(u') - y(-u')]}{\cos u - \cos u'} \frac{du'}{\pi}. \tag{7.26}$$

Similarly, from (7.21c), we get

$$\hat{y}(x) = y_\infty + \int_0^{\pi} \log \left| \frac{2 \sin \frac{1}{2}(u(x) - u(x')) \sin \frac{1}{2}(u(x) - u(-x'))}{\cos x - \cos x'} \right| \frac{dx'}{\pi}. \tag{7.27}$$

These equations have the same general character as the equations worked out for the even-periodic case, to which they quickly reduce if one puts $y(-u') = y(u')$ and $u(-x') = -u(x')$. Although we have not applied these equations to numerical test cases, we see no reason why the methods of interspersed Gaussian quadrature and Newton–Raphson iteration, as already described in detail for the even-periodic case, should not work equally well.

The Theodorsen form (7.25a) is probably of comparable utility to (7.26), but both of these have the limitation already noted in Section III in cases of significant crowding. For most cases, the preferred equation is (7.27).

5. Harmonic Functions and Their Boundary Values

Consider a periodic harmonic function $f(x, y)$ with its boundary value, tangential derivative, and normal derivative along $y = \hat{y}(x)$ specified by $f(x) \equiv f(x, \hat{y}(x))$, $f_s(x)$, $f_n(x)$. The procedure here follows that of Section III.5. We consider the companion functions $df(x)/dx$, $f_{nsq}(x)$ as defined in that subsection. We consider the mapping from R_w as already prescribed and the function $\bar{f}(u) = f(x)$ with the related definitions

$$\bar{f}_s(u) = \frac{df(x)}{dx}\left(\frac{du(x)}{dx}\right)^{-1}, \qquad \bar{f}_n(u) = f_{nsq}(x)\left(\frac{du(x)}{dx}\right)^{-1}.$$

We define an analytic function $F(w)$ in R_w by

$$F(w) = +i\int_{-\pi}^{\pi} \cot\frac{1}{2}(w - u')\,\bar{f}(u')\,\frac{du'}{2\pi}.$$

Then we can identify, by comparison with Eq. (7.7b) and Section (III.5),

$$\bar{f}(u) = F_{\mathrm{R}}(u, 0), \qquad \bar{f}_n(u) = \frac{-\partial F_{\mathrm{I}}(u, 0)}{\partial u},$$

and

$$\left(\frac{i\,dF(w)}{dw}\right)_{v=0} = \bar{f}_n(u) + i\bar{f}_s(u).$$

Exploiting the representations already worked out, we get the relations between boundary values and boundary derivatives of $f(x, y)$ in nonsingular integral representations as follows:

$$f(x) = f_\infty + 2\int_{-\pi}^{\pi} \log|\sin\tfrac{1}{2}(u(x) - u(x'))|\,[f_{nsq}(x') - f_{nsq}(x)]\,dx'/(2\pi) + f_{nsq}(x)[\hat{y}(x) - y_\infty - 2\log 2], \tag{7.28a}$$

with

$$f_\infty = \int_{-\pi}^{\pi} f(x')\,\frac{du(x')}{dx'}\,\frac{dx'}{2\pi}. \tag{7.28b}$$

Also

$$\frac{df(x)}{dx} = \int_{-\pi}^{\pi} \cot\frac{1}{2}(u(x) - u(x'))\left[f_{nsq}(x')\,\frac{du(x)}{dx} - f_{nsq}(x)\,\frac{du(x')}{dx'}\right]\frac{dx'}{2\pi} \tag{7.29}$$

and

$$f_{nsq}(x) = -\int_{-\pi}^{\pi} \cot\frac{1}{2}(u(x) - u(x'))\left[\frac{df(x')}{dx'}\,\frac{du(x)}{dx} - \frac{df(x)}{dx}\,\frac{du(x')}{dx'}\right]\frac{dx'}{2\pi}. \tag{7.30}$$

VIII. Circle Geometry

1. *Correspondence with Periodic Geometry*

The conformal map problem for the interior or exterior of a simply connected bounded region has the same structure as that already treated for a half-plane with periodic boundary. Here, we consider conformal maps onto the exterior of the unit circle. The formulas and methods already developed for periodic geometries can be directly transcribed to the circular case.

We continue to regard the z and w planes as the domains for periodic problems. We gain let R_w denote the upper half strip $-\pi \leqslant u \leqslant \pi$, $0 \leqslant v < \infty$, and let R_z be the image region bounded below by $y = \hat{y}(x)$. Consider also the Z and W complex planes with $Z = X + iY$, $W = U + iV$. Let r, θ be polar coordinates in the Z plane and ρ, ϕ be polar coordinates in the W plane. Consider the transformations

$$Z = -e^{-iz}, \qquad W = -e^{-iw}. \tag{8.1}$$

In terms of coordinates, (8.1) implies

$$r = e^{y}, \theta = \pi - x \qquad \text{and} \qquad \rho = e^{v}, \phi = \pi - u. \tag{8.2}$$

The transformation of z to Z maps R_z onto the region R_+ exterior to the curve

$$r = \hat{r}(\theta) = e^{\hat{y}(\pi-\theta)}.$$

Similarly, R_w is mapped onto the region R_W exterior to the unit circle. The vertical boundaries of R_w are both mapped onto the line, $1 \leqslant U < \infty$, $V = 0$, and the points at ∞ correspond.

Suppose $F(W)$ is an analytic function in the region R_W and converging to $F(\infty)$ as $|W| \to \infty$. From (7.8) and (8.2) we can write

$$F_{\mathrm{R}}(e^{i\phi}) = F_{\mathrm{R}}(\infty) + \text{p.v.} \int_0^{2\pi} \cot \frac{1}{2}(\phi - \phi') F_{\mathrm{I}}(e^{i\phi'}) \frac{d\phi'}{2\pi}, \tag{8.3a}$$

and

$$F_{\mathrm{I}}(e^{i\phi}) = F_{\mathrm{I}}(\infty) - \text{p.v.} \int_0^{2\pi} \cot \frac{1}{2}(\phi - \phi') F_{\mathrm{R}}(e^{i\phi'}) \frac{d\phi'}{2\pi}. \tag{8.3b}$$

Let $Z = Z(W)$ be the conformal map from R_W to R_Z which maps the point $|W| = \infty$ onto the point $|Z| = \infty$. We denote the coordinate transformations by

$$r = r(\rho, \phi) \qquad \text{and} \qquad \theta = \theta(\rho, \phi), \tag{8.4}$$

and the boundary functions by

$$r(\phi) = r(1, \phi) \qquad \text{and} \qquad \theta(\phi) = \phi(1, \phi). \tag{8.5}$$

Thus,

$$r(\phi) = \hat{r}(\theta(\phi)). \tag{8.6}$$

Furthermore, we define r_∞ and θ_∞ by

$$\lim_{\rho\to\infty} r(\rho, \phi) = \rho r_\infty , \tag{8.7a}$$

$$\lim_{\rho\to\infty} \theta(\rho, \phi) = \phi + \theta_\infty , \tag{8.7b}$$

with θ_∞ implicitly determined by the standardization $\theta(0) = 0$. The transformation of Eqs. (7.23) to circular geometry gives

$$\theta(\phi) = \phi + \theta_\infty - \int_0^{2\pi} \cot \frac{1}{2}(\phi - \phi') \log[r(\phi')/r(\phi)] \frac{d\phi'}{2\pi} \tag{8.8}$$

and

$$\log r(\phi) = \log r_\infty + \int_0^{2\pi} \cot \frac{1}{2}(\phi - \phi')[(\theta(\phi') - \phi') - (\theta(\phi) - \phi)] \frac{d\phi'}{2\pi} . \tag{8.9}$$

The third integral equation, in the form (7.27), becomes

$$\log \hat{r}(\theta) = \log r_\infty + \int_0^{\pi} \log \left| \frac{2 \sin \frac{1}{2}[\phi(\theta) - \phi(\theta')] \sin \frac{1}{2}[\phi(\theta) - \phi(-\theta')]}{\cos\theta - \cos\theta'} \right| \frac{d\theta'}{\pi} . \tag{8.10}$$

By (8.2), we have $du/dx = d\phi/d\theta$ relating the measures of crowding in the two schemes. Even if a problem is originally posed in the periodic framework, it may be easier to estimate the character of the mapping function by transforming to the equivalent circle scheme. In circle geometry, the crowding is likely to be proportional to a ratio of the natural geometric parameters that characterize the curve, whereas, as is already suggested by (8.1), exponentials of the natural parameters (e.g., such as D for cosine curves in Section V) come into play in the periodic scheme. Thus, the shifted circle approximation of Section V.2 was motivated by the circle geometry analog.

A single-valued boundary curve in periodic geometry corresponds to a star-shaped region about the origin when transformed to circle geometry. If the region is star shaped about a point other than the origin, then after a translation $W' = W - W_0$ our conformal map procedure may be applied. This has application in hydrodynamics when an interface bends back on itself; e.g., the breaking of a surface (water) wave or the late stage of Kelvin–Helmholtz instability. More generally, a conformal map does not preserve the star-shaped property. As a result, a suitable choice of a "premap" may be used to extend the conformal map procedure to more general regions.

The conformal maps discussed in this paper carry the point at ∞ into the point at ∞. It is worth noting, that more general maps may be convenient for certain potential problems, e.g., in even-periodic geometry when the potential or its normal derivative vanishes on the side boundaries and at ∞. The additional generality can be introduced by considering transformations which leave the boundary of the region invariant. Their form can be inferred from the relation to circle geometry, where, as is well-

known, the general conformal map which takes the exterior of a circle onto itself (while shifting the point at ∞) is

$$W' = e^{i\alpha}(W - \rho)/(1 - \rho^* W),$$

with α real and $| \rho | < 1$.

IX. Linear Geometry

Lastly, we record the basic formulas for linear geometry, which algebraically is the simplest of all.

Suppose $F(w)$ is analytic in the upper-half w-plane and tends to $F(\infty)$ as $| w | \to \infty$ in the region. Then the boundary relations are given by the well-known Hilbert transforms:

$$F_R(u, 0) = F_R(\infty) - \frac{\text{p.v.}}{\pi} \int_{-\infty}^{\infty} \frac{F_I(u', 0)}{u - u'} du', \tag{9.1}$$

$$F_I(u, 0) = F_I(\infty) + \frac{\text{p.v.}}{\pi} \int_{-\infty}^{+\infty} \frac{F_R(u', 0)}{u - u'} du'. \tag{9.2}$$

Let $y = \hat{y}(x)$ be a curve in the z-plane with $\hat{y}(x) \to 0$ as $| x | \to \infty$. Then the three nonsingular integral equations which specify the mapping $z = z(w)$ which carries the part of the z plane above $y = \hat{y}(x)$ onto the upper-half w-plane, according to the scheme of the previous sections, are

$$x(u) = u + x_\infty - \frac{1}{\pi} \int_{-\infty}^{\infty} \frac{y(u') - y(u)}{u - u'} du', \tag{9.3}$$

$$y(u) = \frac{1}{\pi} \int_{-\infty}^{\infty} \frac{x(u') - u' - [x(u) - u]}{u - u'} du', \tag{9.4}$$

and

$$\hat{y}(x) = \frac{1}{\pi} \int_{-\infty}^{\infty} \log \left| \frac{u(x) - u(x')}{x - x'} \right| dx'. \tag{9.5}$$

Again, (9.5) is expected to be the most generally useful of the three for numerical work.

X. Summary

Complex variable techniques have been used to derive a series of integral equations for the determination of conformal transformations in two dimensions. Three of these equations, Eqs. (3.21), (3.22), and (3.23) of the text, have been tested in extensive numerical experiments in the context of even-periodic geometry. The third equation on the list was the most successful, especially in mapping situations with severe crowding,

although the first two were adequate for cases of lesser crowding and for calculation of the mapping in the interior of the region at a lesser level of accuracy. The numerical procedures have been explained in sufficient detail, it is hoped, to make them directly usable by other investigators. The qualitative characteristics of a conformal map in a case of substantial crowding are indicated by Fig. 1, and the quantitative results obtainable from the third integral equation, as regards accuracy, convergence, and computer time have been represented in Tables I through IV. The differential equation for the map function derived in Section VI appears to be a promising approach for problems with time-dependent boundaries as it avoids the necessity for any matrix inversions or Newton–Raphson iterations; we have not yet explored its feasibility, however, in a practical application.

REFERENCES

1. C. ANDERSEN, S. E. CHRISTIANSEN, O. MÖLLER, AND H. TORNHAVE, *in* "Selected Numerical Methods" (C. Gram, Ed.), Chap. 3, Regnecentralen, Copenhagen, 1962 and D. GAIER, Konstruktive Methoden der Konformen Abbildung, Springer-Verlag, Berlin/New York, 1964.
2. DAVID C. IVES, *AIAA J.* **14** (1976), 1006.
3. J. K. HAYES, D. K. KAHANER, AND R. G. KELLNER, *Math. Comput.* **26** (1972), 327.
4. J. K. HAYES, "Four Computer Programs Using Green's Third Formula to Numerically Solve Laplace's Equation in Inhomogeneous Media," Los Alamos Scientific Laboratory Report LA-4423, (1970). This approach was applied in J. HAYES AND R. KELLNER, *SIAM J. Appl. Math.* **22** (1972), 503.
5. R. T. DAVIS, "Methods for Coordinate Generation and Potential Flow Solution Based on Schwarz–Christoffel Transformation," American Institute of Aerodynamics and Astrodynamics, Williemsburg, Va., July 24, 1979, Paper No. 79-1463.